

Neuron-Glial Interactions

Maurizio De Pittà
Basque Center for Applied Mathematics, Bilbao, Spain
mdepitta@bcamath.org

April 11, 2020

Accepted for publication in the *Encyclopedia of Computational Neuroscience*, D. Jaeger and R. Jung eds., Springer-Verlag New York, 2020 (2nd edition).

Neuron-Glial Interactions

Maurizio De Pittà
Basque Center for Applied Mathematics, Bilbao, Spain
mdepitta@bcamath.org

April 11, 2020

Synonyms

neuron-glial interaction modeling, synapse-astrocyte bidirectional signaling, axon-glial signaling, microglia modeling, computational glioscience

Definition

Dependence of neuronal function on glial cells and vice versa, which consists of the interplay of potentially multiple signals that can be both of neuronal and of glial origin. This interplay may be facilitated by the specific arrangement of neurons vs. glia in different brain areas and occurs on time scales extending from milliseconds to months, as well as on spatial scales ranging from subcellular and synaptic levels to those of networks and whole-brain structures.

Contents

1	Introduction	4
2	Anatomy of neuron-glia interactions	5
2.1	Myelination of axons by oligodendrocytes	5
2.2	Müller glia in the retina	5
2.3	Astrocytes and regulation of volume transmission	6
3	Physiology of neuron-glia interactions	7
3.1	General modeling framework	7
3.2	Modulation of neural excitability	12
3.3	Neuron-glia interactions in neural networks	13
3.4	Regulation of synaptic transmission and plasticity	14
3.5	Glial cytokine signaling	17
4	Temporal and spatial scales of neuron-glia interactions	18
4.1	Morphology and structural plasticity	18
4.2	Calcium signaling	19
4.3	Glutamate-glutamine cycle and astrocyte-to-neuron lactate shuttle	20
4.4	Gliotransmission	21
4.5	Ion homeostasis	21
4.6	Regulation of the blood flow	22
5	Conclusion	22
6	Acknowledgments	22
7	Cross-references	22

1 Introduction

Most animals share the ability to move in response to external stimuli, which results from having developed complex neural structures that allow for sophisticated processing of sensory information. From a phylogenetic perspective, as the nervous system changed from a simple net-like structure, such as in jellyfish (*Cnidara*), to condensed ganglia and centralized brains – starting with flat interstitial worms (*Acoelomorpha*) up to mammals (*Chordata*)–, a new cell type could be recognized in morphological studies: glial cells (Hartline, 2011; Laming et al, 2000). The importance of this new cell type for a functional brain is arguably reflected by the increase in the relative number of glial cells during evolution: there are roughly equal numbers of glial cells and neurons in mammals (Herculano-Houzel, 2014) whereas, by contrast, glia constitutes only 10% of invertebrate neural cells in *Drosophila* or *C. elegans* (Hartline, 2011; Bullock and Horridge, 1965).

It is currently unknown whether glial cells from different clades share similar functions: the molecular, morphological, and physiological identity of glial cells across and within clades indeed remains a topic of active investigation (Hartline, 2011). In the mammalian brain, the most numerous glial cells appear to fall into two categories: (i) macroglia, which is prominently constituted of oligodendrocytes and astrocytes, and (ii) microglia (Lawson et al, 1990; Pelvig et al, 2008). Significantly, despite their different developmental origin – macroglia originating from the embryonic ectoderm while microglia coming from the mesoderm –, both cell types share a common feature: that is physical proximity to neurons by an elaborated branched anatomy that interweaves with neural processes (Kettenmann and Ransom, 2013). This feature can be regarded as the teleological evidence of the purpose of glia for being an integral part of both the structure and function of neural networks of the mammalian brain.

Oligodendrocytes, for example, are responsible for myelination of axons, which is essential for their trophic support to attain long lengths while allowing for evolved organisms, like mammals and vertebrates in general, to achieve great sizes (Nave, 2010). At the same time, myelination provides axons with high membrane electrical resistance and low capacitance, which prevents current loss and enables rapid and efficient conduction of action potentials – a prerogative of complex nervous systems to operate quickly and efficiently (Zalc and Colman, 2000). As nervous systems increase in complexity, and this complexity correlates with the increasing sophistication of neurological function, a trend in increased complexity is also observed for astrocytes (Verkhatsky and Nedergaard, 2016). Humans and primates indeed possess astrocytes that are larger and more branched than rodent astrocytes, with humans astrocytes generally being the largest (Oberheim et al, 2009). In agreement with this trend, if we graft human astrocytes in mice, we get animals that show enhanced learning and memory capabilities (Han et al, 2013). Finally, microglia, too, can be framed within the evolutionary perspective, in connection with the appearance of compact neural masses and the increased demand thereby of specialized phagocytic and immune functions, including mechanisms of neural protection (Pósfai et al, 2019). Remarkably, microglia invades the neural tube during embryogenesis before epithelial cells, neurons, and macroglia, being in the ideal position to regulate angiogenesis as well as neuro- and gliogenesis. It is now emerging that such regulation could extend beyond embryonic life as microglia can promote the formation and dismantling of functional neuron-glia networks by axon reorganization during development and by regulation of genesis and pruning of synapses in the mature brain (Pósfai et al, 2019).

Although lagging behind classical computational neuroscience, theoretical and computational approaches are beginning to emerge to characterize different aspects of neuron-glia interactions (De Pittà and Berry, 2019a). This chapter aims to provide essential knowledge on neuron-glia interactions in the mammalian brain, leveraging on computational studies that fo-

cus on structure (anatomy) and function (physiology) of such interactions in the healthy brain. Although our understanding of the need of neuron-glia interactions in the brain is still at its infancy, being mostly based on predictions that await for experimental validation, simple general modeling arguments borrowed from control theory are introduced to support the importance of including such interactions in traditional neuron-based modeling paradigms.

2 Anatomy of neuron-glia interactions

2.1 Myelination of axons by oligodendrocytes

Myelination by oligodendrocytes and axon growth seem to be entirely interdependent since there are direct relationships among the age at which axons are myelinated, their final diameter in the adult, and the development of the associated oligodendrocytes (Butt, 2013). Accordingly, oligodendrocytes and their axons should be considered together as functional units rather than separate functional entities. Myelinated axons can thus be thought to be functionally specialized since internodes provided by myelinic ensheathing, and nodes of Ranvier develop in a concerted fashion to fulfill specific computational tasks (Tomassy et al, 2016; Hughes et al, 2018).

Electrical cable theory (FitzHugh, 1962; Goldman and Albus, 1968; Moore et al, 1978; Waxman, 1980; Richardson et al, 2000) predicts that regulation of myelin thickness, internode length and node geometry by oligodendrocytes (Ullén, 2009; Fields, 2008; Arancibia-Carcamo et al, 2017) could account for fine-tuning of action potential (AP) shape and conduction velocity (Kimura and Itami, 2009; Tomassy et al, 2014; Ford et al, 2015; Hughes et al, 2018) with important functional consequences. For instance, variations of internodal length associated with axon diameter dictate the extent of co-activation of nodal Na^+ with low-threshold K^+ channels. In turn, a triaxial cable model of myelinated axons in sound processing circuits reveals how the synchronous activation of these channels may account for large, fast-rising and brief APs, differentiating axons that can propagate APs at high rates, and that belong to neurons that encode for high-frequency sounds, from axons that cannot, and instead depart from neurons that respond to low-frequency sounds (Halter and Clark Jr., 1991; Ford et al, 2015). In those circuits, adjustments of internodal length may also occur in close register with nodal diameter, crucially setting the timing of AP arrival at synaptic terminals, which, in turn, underpins precise binaural processing of temporal information for sound localization (Carr and Konishi, 1990; Carr et al, 2001; Carr and Soares, 2002; McAlpine and Grothe, 2003; Seidl et al, 2010; Ford et al, 2015). Together with delays induced by the AP-generation dynamics (Fourcaud-Trocmé et al, 2003) and those rising from synaptic processing (Markram et al, 1997), axonal conduction delays due to myelination by oligodendrocytes are an important property of neural interactions, which may induce a wealth of dynamical states with different spatiotemporal properties and domains of multistability that could serve different computational purposes (Roxin et al, 2005; Roxin and Montbrió, 2011).

2.2 Müller glia in the retina

Formation of axon-myelin units by oligodendrocytes to fulfill specific functional tasks is only one of the possibly many cases of how neuronal structures and glial cells' morphology develop in a tight association. Another example is the retina of the vertebrate eye. Notably, this structure is inverted with respect to its optical function so that light must pass through several tissue layers before reaching the light-detecting photoreceptor cells. In doing so, projected images on the retina would rapidly deteriorate due to light scattering by optical and geometrical inhomogeneities of those different layers if it were not for specific properties and arrangement of structures and cell assemblies of the retina that ensure correct vision (Tuchin, 2000; Masland,

2001). In this scenario, the most common type of retinal glial cells, known as Müller cells, show a characteristic cylindrical, funnel-like shape that spans the entire thickness of the retina and functions as the waveguide of visible light from the retinal surface to the photoreceptor cell layer (Franze et al, 2007). Numerical solution of the Helmholtz equation in a model of retinal tissue suggests that this property of Müller cells to guide light crucially enhances vision acuity since, like fiber optics that penetrate through the retinal layers, these cells can propagate light straight down to the photoreceptor cell they associate with (Labin and Ribak, 2010). In particular, every mammalian Müller cell is coupled, on average, to one cone photoreceptor cell, that is responsible for sharp seeing under daylight conditions (i.e., photopic vision), plus several rod photoreceptor cells, serving low-light-level, night (scotopic) vision (Reichenbach and Robinson, 1995). Remarkably, the spectrum of light transmitted through Müller cells, derived from theoretical calculations based on data of the human parafoveal retina, matches almost perfectly the absorption spectra of the medium- and long-wavelength human cone photoreceptors, predicting a gain in photon absorption by a factor of ~ 7.5 by these photoreceptors, and by a factor of ~ 4 by human short-wavelength cones (Labin et al, 2014). At the same time, the spectrum of light leaking outside Müller cells matches the absorption spectrum of human rod photoreceptors. In this fashion, Müller cells provide a mechanism to improve cone-mediated photopic vision, with minimal interference with rod-mediated scotopic vision since not only they guide light of relevant wavelengths for cone visual pigments directly towards cones, but also they allow for light of wavelengths more suitable for rod vision to leak to surrounding rods (Labin et al, 2014).

2.3 Astrocytes and regulation of volume transmission

Broadly speaking, the factors underpinning morphogenesis of neuronal structures in tight association with glial cells remain poorly understood, although they are thought to encompass a combination of transcriptional programs and a battery of molecular signals that seem to be regulated both developmentally and regionally, in a cell-specific manner (Jadhav et al, 2009; Eroglu and Barres, 2010; Götz, 2013; Stassart et al, 2013). A paramount example of this complex combination of factors is provided by astrocytes, which are glial cells predominantly found in the cortex and hippocampus and are recognized as critical regulators of the neuronal connectome in those brain regions (Fields et al, 2015). In the postnatal, developing brain, astrocytes are indeed found in spatially distinct domains and express domain-specific genes that are needed to support the formation of specific neural circuits and neuronal subtypes (Molofsky et al, 2014). On the other hand, they also secrete a variety of molecules that regulate with spatiotemporal specificity all stages of the genesis of functional neural circuits, such as the establishment of immature (silent) synapses between axon and dendrites, the conversion of these silent synapses into active ones by insertion (and maintenance) of functional receptors, and the elimination of excess synapses and synaptic pruning to refine connections in neural circuits (Allen, 2013; Clarke and Barres, 2013). Remarkably, this close relationship between astrocytes and synapses continues in the adult brain, with the processes of astrocytes that infiltrate into the neuropil and wrap themselves around synapses in a seemingly non-random fashion (Reichenbach et al, 2010), engaging in a multitude of signals (Figure 1), with figures approaching 20–180 thousand synapses contacted by a single astrocyte in the rodent brain (Bushong et al, 2002), but ~ 270 thousand to 2 million synapses per astrocyte in the human brain (Oberheim et al, 2009). What are the possible functional purposes of this ensheathing?

One obvious possibility is that processes of astrocytes are strategically positioned at synaptic loci to act as physical barriers that constrain and regulate extracellular diffusion of neurotransmitters (Ventura and Harris, 1999). With this regard, a realistic reconstruction of the extracellular space (ECS) in between astrocytic processes and glutamatergic synapses of the

hippocampus – one of the brain structures where the morphological association of astrocytes with synapses has been best-characterized (Seifert and Steinhäuser, 2017) – revealed a strong anisotropy for glutamate diffusivity, directly imputable to the peculiar arrangement of astrocytes with the surrounding neuropil (Kinney et al, 2013). This anisotropy ensues from the nonuniform width of ECS, which forms thin sheets in the periastrycytic space and grows wider into tunnels in correspondence with synapses and axons. Monte Carlo diffusion simulations show that the diffusion rate of glutamate through the neuropil critically depends on the proportion of sheets vs. tunnels, since the smaller median extracellular width of astrocyte-delimited sheets, poses a diffusion barrier to glutamate molecules, corralling them into tunnels which favor their diffusion instead (Kinney et al, 2013). This scenario, along with the expression of glutamate transporters by perisynaptic astrocytic processes (Danbolt et al, 2002), would ultimately provide a mechanism to canalize glutamate to specific targets while keeping low the risk of excitotoxicity brought forth by the fact that glutamate is not normally destroyed in the ECS (Rothstein et al, 1996).

The degree of astrocytic ensheathing at glutamatergic synapses indeed directly dictates the rate of glutamate uptake by glial transporters – the primary mechanism of glutamate uptake in the adult brain (Danbolt, 2001) –, regulating the time course of this neurotransmitter in the synaptic cleft, and its potential to spill out to neighboring synapses (Clements, 1996). Remarkably, the degree of astrocyte ensheathment seems inversely correlated with the size of dendritic spines (Medvedev et al, 2014), suggesting that, in agreement with independent theoretical arguments (Barbour, 2001), smaller synapses are best sealed by astrocytic processes to minimize glutamate spillover. On the contrary, glutamate spillover could occur at larger synapses, for which the degree of astrocytic ensheathing is only up to approximately one-third of their perimeter (Ventura and Harris, 1999). To the extent that thin-spine vs. large-spine synapses can respectively be assimilated to silent vs. functional synapses (Matsuzaki et al, 2001), the latter possibility hints a crucial role of astrocytic ensheathing in the regulation of glutamate clearance at functional excitatory synapses, with the potential to regulate independent synaptic activation vs. synaptic cross-talk (Huang and Bergles, 2004).

3 Physiology of neuron-glia interactions

3.1 General modeling framework

If the reciprocal disposition of neurons with respect to glial cells in the brain fulfills essential anatomical constraints for their interaction, the existence of two-way dynamic signaling, from neurons to glia and vice versa, accounts for the physiology of this interaction. With this regard, a common framework to model networks of interacting neurons (Ermentrout and Terman, 2010) may be borrowed to illustrate essential functional consequences of neuron-glia interactions. Denoting by \mathbf{x} and γ the activities of neuronal and glial interacting ensembles, respectively defined as column vectors in \mathbb{R}^N and \mathbb{R}^G , then the glial activity can generally be described by

$$\tau_\gamma \dot{\gamma} = -\gamma + \mathcal{F}_\gamma(\mathbf{b}_\gamma + \mathbf{I}_\gamma(\mathbf{x}, \gamma)) \quad (1)$$

where $\mathcal{F}_\gamma : \mathbb{R}^g \rightarrow \mathbb{R}^G$ ($g \geq G$) represents the glial input-output transfer function. The argument of this function – that is the input to glia – consists of (i) an external bias $\mathbf{b}_\gamma \in \mathbb{R}^g$ coming, for example, from brain areas away from the neuron-glia ensemble under consideration, and of (ii) a recurrent input $\mathbf{I}_\gamma(\mathbf{x}, \gamma) : \mathbb{R}^{N+G} \rightarrow \mathbb{R}^g$ due to neuronal and glial activities within the ensemble itself. The physiological correlate of γ , along with the choice of \mathcal{F}_γ and \mathbf{I}_γ depend on what “glial activity” refers to, and it will be clarified as follows. Similarly, without specifying

for now what “neuronal activity” is, an equation analogous to **1** may be written for \mathbf{x} , i.e.

$$\tau_x \dot{\mathbf{x}} = -\mathbf{x} + \mathcal{F}_x(\mathbf{b}_x + \mathbf{I}_x(\mathbf{x}, \gamma)) \quad (2)$$

where $\mathcal{F}_x : \mathbb{R}^n \rightarrow \mathbb{R}^n$, $\mathbf{b}_x \in \mathbb{R}^n$ and $\mathbf{I}_x(\mathbf{x}, \gamma) : \mathbb{R}^{N+G} \rightarrow \mathbb{R}^n$ ($n \gtrsim N$). In the previous equations, what the “activities” \mathbf{x} and γ refer to are suitable measurables of neuronal and glial physiology, respectively. Membrane voltage, firing rate, and synaptically-released neurotransmitters are typical examples of such measurables for neurons. For glia instead, cytosolic calcium is probably the most hitherto studied readout of these cells in response to neuronal stimulation, yet possibly not the only one, since other intracellular ions like Na^+ , K^+ , H^+ , Cl^- or HCO_3^- , along with a whole cassette of molecules involved in the genesis of calcium signaling, could also be indicators of glial stimulation (De Pittà and Berry, 2019b). At the same time, the notion of neuronal and glial ensembles is somehow broad. We may encompass by this notion brain structures, including whole networks of neurons and glia, or components of these networks, for example, myelinated axons with their oligodendrocytes, or groups of synapses with their perisynaptic glial processes (of astrocytic or microglial origin). In this context, the emerging notion that calcium homeostasis, as well as the homeostasis of other ions and macromolecules, could be compartmented within the glial cell’s morphology (Breslin et al, 2018, see also **ref.** COMPUTATIONAL MODELING OF INTRACELLULAR ASTROCYTE CA^{2+} SIGNALS), allows using equations akin to **1** and **2** to model dynamics of neuron-glia interactions at multiple spatial scales, where scale-specific aspects of such interactions may be lumped into the choice of the transfer functions \mathcal{F}_i (with $i = \mathbf{x}, \gamma$), their input arguments \mathbf{b}_i , \mathbf{I}_i , and ultimately, the components of the activity vectors \mathbf{x} and γ .

The functions \mathcal{F}_i and \mathbf{I}_i are generally nonlinear with respect to their input variables. This hinders any attempt to look beyond the general form of equations **1** and **2** to fathom neuron-glia interactions with the aim to derive different mechanisms of action and function that could be shared (or not) by different pathways of interaction. The situation greatly simplifies if we limit our analysis to the first order expansion of \mathbf{I}_i around the resting point (\mathbf{x}_0, γ_0) . In this case, equations **1** and **2** become

$$\tau_\gamma \dot{\gamma} \approx -\gamma + \mathcal{F}_\gamma(\mathbf{b}_{0_\gamma} + \mathbf{W}_x(\mathbf{x} - \mathbf{x}_0) + \mathbf{J}_\gamma(\gamma - \gamma_0)) \quad (3)$$

$$\tau_x \dot{\mathbf{x}} \approx -\mathbf{x} + \mathcal{F}_x(\mathbf{b}_{0_x} + \mathbf{J}_x(\mathbf{x} - \mathbf{x}_0) + \mathbf{W}_\gamma(\gamma - \gamma_0)) \quad (4)$$

where, for $i = \mathbf{x}, \gamma$, $\mathbf{b}_{0_i} = \mathbf{b}_i + \mathbf{I}_i(\mathbf{x}_0, \gamma_0)$, $\mathbf{J}_i = (D_i \mathbf{I}_i(i, j))_{(\mathbf{x}_0, \gamma_0)}$ and $\mathbf{W}_i = (D_j \mathbf{I}_i(i, j))_{(\mathbf{x}_0, \gamma_0)}$, with $D_x \mathbf{I}_i = \left(\frac{\partial \mathbf{I}_i}{\partial x_0}, \dots, \frac{\partial \mathbf{I}_i}{\partial x_{N-1}} \right)$ and $D_\gamma \mathbf{I}_i = \left(\frac{\partial \mathbf{I}_i}{\partial \gamma_0}, \dots, \frac{\partial \mathbf{I}_i}{\partial \gamma_{G-1}} \right)$. In this way, it is possible to distinguish between different contributions to the evolution of neuronal (glial) activity by \mathcal{F}_x (\mathcal{F}_γ), in particular separating those that are due to neuronal (glial) elements weighted by the matrix \mathbf{J}_x (\mathbf{J}_γ) from those that ensue instead from glial (neuronal) elements and are weighted by the matrix \mathbf{W}_x (\mathbf{W}_γ). Because matrices \mathbf{J}_x , \mathbf{J}_γ lump couplings of neuronal (respectively glial) activities with themselves, whereas matrices \mathbf{W}_x , \mathbf{W}_γ couple neuronal activities with glial activities and vice versa, we hereafter refer to them as *homotypic* and *heterotypic* weight (or connection) matrices, respectively.

The input terms associated with heterotypic connections represent the actual interaction pathways, for signaling from neurons to glia ($\mathbf{W}_x \mathbf{x}$), and vice versa, from glia to neurons ($\mathbf{W}_\gamma \gamma$). In several practical scenarios (Figure 2), this signaling is mediated by specific molecules or ions, that may themselves be regarded as measures of neuronal (glial) activity, or can alternatively be expressed in terms of \mathbf{x} (respectively γ). Consider for example synaptically-evoked gliotransmission (Araque et al, 2014, see also *yellow* and *red* pathways in Figure 1). This form of neuron-glia interaction consists of the activity-dependent release of neuroactive molecules from astrocytes,

including neurotransmitters like glutamate, ATP, GABA, or D-serine that, for their glial origin, are termed “gliotransmitters.” The release can be triggered by synaptically-released neurotransmitters and be mediated by different intracellular pathways that often associate with transient calcium signaling in the astrocyte (Savtchouk and Volterra, 2018). In turn, gliotransmitters can modulate synaptic transmission both presynaptically – binding to receptors that regulate the probability of release of neurotransmitter-containing synaptic vesicles –, and postsynaptically, gating receptors/ion channels that control neuronal depolarization (and excitability). In this description, synaptically-released neurotransmitters mediate neuron-to-astrocyte signaling, whereas gliotransmitters are responsible for the astrocyte-to-neuron signaling. To couple these two signaling pathways by the above framework, however, biophysical correlates for their functional interdependence must also be explored. For the dependence of gliotransmitter release on synaptic release, at least at first approximation, gliotransmitter release is expected to rise with synaptic neurotransmitter release (Araque et al, 2014). For the dependence of this latter on gliotransmitter release instead, the reasoning is as follows: (i) activation of presynaptic receptors by gliotransmitters increases with gliotransmitter release; in turn (ii) modulation of intrasynaptic Ca^{2+} , which is linked with p – the synaptic release probability (**ref.** CALCIUM-DEPENDENT EXOCYTOSIS, BIOPHYSICAL MODELS) –, correlates with the degree of receptor activation by gliotransmitters; (iii) synaptic release is proportional to p . In this fashion, the simplest scenario sees γ in the above equations reducing to a scalar variable that is associated with the fraction of gliotransmitter-activated receptors, whereas p replaces \mathbf{x} . Then, assuming that at rest $\gamma_0 = 0$, $p_0 = p^* > 0$, the simplest model for the presynaptic pathway of synaptically-evoked gliotransmission (Figure 2A) derived by equations 3 and 4 reads

$$\tau_\gamma \dot{\gamma} = -\gamma + \mathcal{F}_\gamma (b_{\gamma_0} + W_\gamma p + J_\gamma \gamma) \quad (5)$$

$$\tau_p \dot{p} = p^* - p + \mathcal{F}_p ((1 - J_p)p^* + J_p p + W_p \gamma) \quad (6)$$

where b_{γ_0} may or not be present, depending on the presence or not of other mechanisms triggering gliotransmitter release that are independent of stimulation of the very synapse modulated by gliotransmission, e.g., microglia-mediated Ca^{2+} signaling in the astrocyte (Pascual et al, 2011). The homotypic weight J_γ accounts for the theoretically-predicted phenomenon of gliotransmitter-triggered gliotransmission (Larter and Craig, 2005), whereas the homotypic weight J_p can generally be accounted by mechanisms of short-term plasticity (**ref.** SHORT TERM PLASTICITY, BIOPHYSICAL MODELS). With regard to the heterotypic weights instead, it generally is $W_\gamma > 0$ regardless of the nature of synaptic neurotransmitters, that is both excitatory and inhibitory neurotransmitters are excitatory for glial activation (Durkee et al, 2019). The sign of W_p instead is dependent on the nature of gliotransmission, which can either decrease or increase synaptic release (De Pittà et al, 2015). Remarkably, while the sign of W_p is set by functional and anatomical features of synapse-astrocyte ensembles (De Pittà, 2019), the further possibility that the polarity of gliotransmission could also depend on specific patterns of activity (Covelo and Araque, 2018) can be accounted by the choice of \mathcal{F}_p .

If we aim for a more general understanding of gliotransmission on synaptic transmission, it is then useful to think of the efficacy (or strength) of synaptic transmission in terms of the product $w = p \cdot q$, where q is the probability of activation of postsynaptic receptors by the presynaptically released neurotransmitter. In this context then, choosing $\mathbf{x} = (p, q)^T$ with $q_0 = q^* > 0$, results in the system of three equations in the general form of

$$\tau_\gamma \dot{\gamma} = -\gamma + \mathcal{F}_\gamma (b_{\gamma_0} + W_\gamma^{(p)} p + W_\gamma^{(q)} q + J_\gamma \gamma) \quad (7)$$

$$\tau_p \dot{p} = p^* - p + \mathcal{F}_p ((1 - J_p)p^* - W_p^{(q)} q^* + J_p p + W_p^{(q)} q + W_p^{(\gamma)} \gamma) \quad (8)$$

$$\tau_q \dot{q} = q^* - q + \mathcal{F}_q (-W_q^{(p)} p^* + (1 - J_q)q^* + W_q^{(p)} p + J_q q + W_q^{(\gamma)} \gamma) \quad (9)$$

The coupling factors J_q , $W_\gamma^{(q)}$, $W_p^{(q)}$ and $W_p^{(\gamma)}$ ensue from the consideration of endocannabinoid signaling, which may retrogradely suppress synaptic activity while, at the same time, triggering Ca^{2+} -dependent gliotransmitter release from the astrocyte (Navarrete et al, 2014). In particular, because this signaling pathway depends on postsynaptic depolarization (v_m), and this latter is dependent on incoming synaptic activity by w , it is safe to assume that endocannabinoid signaling can be expressed in terms of p and q by a proper choice of the transfer functions \mathcal{F}_γ , \mathcal{F}_p , \mathcal{F}_q and their input arguments I_γ , I_p , I_q in the original equations 1 and 2 (Figures 2C,D). On the other hand, when no retrograde signaling (including endocannabinoid) is taken into account, then $J_q = 0$ and also $W_\gamma^{(q)} = W_p^{(q)} = W_p^{(\gamma)} = 0$, allowing for a significant simplification of the above equations. Even more so if the analysis is restricted to the sole postsynaptic pathway of gliotransmission without considering any mechanism of short-term plasticity, for which, synaptic dynamics reduces to $\tau_p \dot{p} = p^* - p$ and $\tau_q \dot{q} = q^* - q + \mathcal{F}_q(-W_q^{(p)} p^* + q^* + W_q^{(p)} p + W_q^{(\gamma)} \gamma)$ with γ being described by an equation like 5. In this scenario gliotransmission release (γ) becomes uncoupled from q (but not the opposite), and the dynamics of both γ and q is driven by p (Figure 2B). The resulting $q(t)$ can essentially be expressed in terms of $p(t)$ but, differently from a stand-alone synapse, the effect of p on q (and thus on v_m) also incorporates, possibly in a nonlinear fashion, the effect of gliotransmission. Remarkably, this scenario could underpin several examples of neuron-glia interactions such as: (i) regulation of long-term synaptic plasticity by D-serine released from astrocytes in the hippocampus, hypothalamus and the cortex (Bains and Oliet, 2007); (ii) AMPA receptor internalization in the cerebellum by D-serine originating from Bergmann glial cells (Kakegawa et al, 2011); (iii) AMPA receptor insertion by adrenergic stimulation of ATP release from hypothalamic astrocytes (Gordon et al, 2005); (iv) modulation of AMPA and GABA receptor trafficking by astrocytic $\text{TNF}\alpha$ (Stellwagen et al, 2005); and (v) slow inward and outward currents (SICs and SOC) respectively mediated by glutamate and GABA from astrocytes (Fellin et al, 2004; Le Meur et al, 2012).

The distinction between homotypic vs. heterotypic couplings brought forth by equations 3 and 4 allows the analysis of otherwise complex neuron-glia interactions in terms of combinations (to the first-order approximation) of feedback and feedforward mechanisms, which can conveniently be illustrated by functional diagrams such as those in Figure 2. Furthermore, consideration of these diagrams can help classify different pathways of interaction between neurons and glia based on their coupling mechanisms. In this fashion, activity-dependent presynaptic pathways of gliotransmission can all be assimilated to a feedback mechanism on synaptic release, which can be either positive or negative, depending, as previously stated, on the nature of astrocyte-synapse coupling and synaptic dynamics (Figure 2A). Conversely, the postsynaptic pathway of gliotransmission is tantamount to a feedforward mechanism on postsynaptic membrane depolarization, which can also be positive or negative, depending on the gliotransmitter type and whether gliotransmission promotes receptor internalization or insertion (Figure 2B). Consideration of endocannabinoid signaling does not change the essence of these mechanisms, except for the fact that a further intermediate processing stage must be taken into account for the regulation of endocannabinoid release from postsynaptic terminals (Figure 2C). Nonetheless, differently from other pathways of synaptic transmission, in this latter case, postsynaptic pathways of gliotransmission may also feedback on endocannabinoid release since this process depends on postsynaptic depolarization (Figure 2D). On the other hand, glutamatergic gliotransmission could also contemplate the existence of positive feedback on the astrocyte by its release of the cytokine $\text{TNF}\alpha$ (Figure 2E). Constitutive extracellular levels of this cytokine ($[\text{TNF}\alpha]_e$) may indeed promote glutamate release from astrocytes but can also regulate the production of $\text{TNF}\alpha$ by these cells (Santello et al, 2011). Furthermore, microglia could also regulate glutamatergic gliotransmission, releasing ATP as part of their immune response, and thereby promoting Ca^{2+} -dependent glutamate release from astrocytes (Pascual et al, 2011).

Alternatively, extracellular glutamate ($[\text{Glu}]_e$) may trigger the release of $\text{TNF}\alpha$ from microglia, which could stimulate the further release of glutamate from astrocytes in, yet another, positive feedback fashion (Bezzi et al, 2001).

Potassium ion homeostasis is also involved in multiple feedback pathways mediated by glia (Figure 2F). Neuronal activity results in local accumulations of extracellular K^+ ($[\text{K}^+]_e$) that may promptly be abated by spatial buffering by glia (Kofuji and Newman, 2004). Significantly, synaptically-evoked Ca^{2+} signaling in astrocytes (*yellow pathway*) can also regulate $[\text{K}^+]_e$ to modulate both spontaneous synaptic release at excitatory synapses and neuronal firing (Wang et al, 2006). In the cerebellum, Ca^{2+} -dependent K^+ uptake by Bergman glia can dramatically alter the firing dynamics of Purkinje cells (Wang et al, 2012b). At cortical axons instead (Figure 2L), depolarization of myelinating oligodendrocytes following AP conduction is speculated (Debanne et al, 2011) to alter extracellular levels of K^+ and Na^+ locally, at nodes of Ranvier, thereby transiently promoting action potential generation which could speed up AP conduction by 10% (Yamazaki et al, 2007). On the other hand, astrocytes, too, could influence AP generation at nodes of Ranvier, specifically by increasing AP duration by Ca^{2+} -dependent glutamate release, although the activity requirements for this pathway are not known (Sasaki et al, 2011).

Very often, a signaling pathway or a biophysical process may be shared by different mechanisms of neuron-glia interactions. Extracellular glutamate and its uptake by astrocytes, for example, are key components of the so-called glutamate–glutamine cycle (GCC), as well as of the astrocyte-to-neuron lactate shuttle (ANLS) (see **ref.** BRAIN ENERGY METABOLISM). In the GCC (Figure 2G), glutamate taken up by astrocytic transporters is converted into glutamine, which is transported back to neurons, where it is presumably reconverted to glutamate, thereby guaranteeing the supply of this neurotransmitter to sustain synaptic transmission (Xiang et al, 2003). In the ANLS instead (Figure 2H), astrocytic lactate – ensuing from ATP demand to counteract intracellular Na^+ accumulation by glutamate uptake –, is shuttled to neurons where it is converted to pyruvate, which is necessary for ATP synthesis by mitochondria, and thus it mediates a positive feedback loop that can sustain the energetic cost of prolonged neuronal firing activity (Allaman et al, 2011). Remarkably, both ANLS and GCC could also be integral components of other pathways of neuron-glia interactions. Lactate, for example, may also cover synaptic energy demand indirectly by triggering prostaglandin release from astrocytes, which, in turn, increases blood flow and thereby, glucose supply to neurons (Attwell et al, 2010). Alternatively, it could also operate as gliotransmitter (Tang et al, 2014). Glutamine produced by GCC, on the other hand, could also be a precursor of glutathione (GSH) in the synthesis of this latter by astrocytes (Figure 2J), which is a key process in neuroprotection by glia. Neurons are also capable of synthesizing GSH from glutamate, but this is constrained by their intracellular availability of cysteine and glycine. Astrocytes can, however, backup on the availability of these two amino acids in neurons by releasing GSH, which is extracellularly cleaved to produce cysteinylglycine that neurons, in turn, cleave to supply cysteine and glycine to their intracellular resources (Dringen, 2000). Finally glutathione metabolism could also be linked with vitamin C (ascorbic acid) exchange between neurons and glia as illustrated by the *brown pathway* in Figure 1 (Castro et al, 2009; May, 2012).

In several cases, neuron-glia interactions add to existing neuronal feedback mechanisms. Two examples, respectively, are the control of extracellular pH and the regulation of blood flow by astrocytes. Neuronal electrical activity results in extracellular alkalization and intracellular acidification around neuronal cell walls, which can considerably alter neuronal excitability and synaptic currents (Deitmer and Rose, 1996). This is put in place by a multitude of diverse mechanisms that rely on physiochemical buffers, metabolic reactions, and membrane transport systems within neurons and in the interstitial fluid that make extracellular and intracellular neuronal pH completely interdependent. On the other hand, intracellular pH of astrocytes

is also dependent on extracellular pH, and astrocytes, akin to neurons, express a variety of transport and buffering mechanisms that make them capable of influencing H^+ homeostasis locally and brain-wide actively. By similar arguments, both neurons and glial cells require a constant supply of metabolites and chemical species by the bloodstream. Yet, they can regulate blood flow by the independent release of vasoactive signals (Attwell et al, 2010), as well as do so in interaction with each other by the other neuron-astrocyte interaction pathways hitherto presented.

The existence of feedback and feedforward pathways of interactions between neuronal and glial elements challenges traditional connectomics. We come to realize in fact that neurons are not merely connected by synapses but also by extracellular glial-mediated pathways. Moreover, for some of these pathways, like at synapses where signal transmission is traditionally assumed to occur in one direction only – from the presynaptic terminal to the postsynaptic one –, this directionality is replaced by a neuron-glial signaling network that is inherently recurrent. Recurrent connections are essential in network theory since they can control the stability of network activity and its robustness to noise. Accordingly, the model of an autaptic neuronal oscillator may conveniently be adopted to get a flavor of the potential relevance of glia-mediated synaptic recurrence on neuronal firing (Volman et al, 2007). The autaptic oscillator consists of an excitatory neuron that exhibits periodic firing employing self-synapses (i.e., autapses) whose strength critically controls the neuron’s firing rate and its stability (Seung et al, 2000). In this fashion, when all autapses also stimulate the same astrocytic domain and are equally affected by release-decreasing gliotransmission ensuing from it, activity-dependent fluctuations of neuronal firing rate emerge in phase opposition with astrocytic Ca^{2+} spikes (Volman et al, 2007). The mechanism would not be surprising *per se* if it were not for the fact that it can also be observed in the presence of irregular bursting by the autaptic neuron. The theory of autaptic oscillators (without astrocyte) predicts in fact that the positive feedback exerted by excitatory autapses on the neuron only allows this latter to maintain its firing rate at the onset of stimulation, or to increase it, ultimately reaching unrealistic (epileptiform) firing rates (Seung et al, 2000). This scenario is avoided in the presence of release-decreasing gliotransmission, however, because any self-amplifying increase of neuronal activity that could be triggered, for example, by a burst of APs, promotes gliotransmitter release from the astrocyte, which promptly counteracts the neuron’s runaway by excitation by depressing autaptic transmission. In this fashion, the negative feedback exerted by gliotransmission on synapses competes with the positive autaptic feedback to prevent the neuron from persistently generating APs at high rates. Rather, the opposite happens, as prolonged periods of depressed synaptic excitation, consistent with the long-lasting effect of release-decreasing gliotransmission observed *in vitro* (Araque et al, 1998), substantially modify the firing statistics of the autaptic neuron, accounting for large interspike intervals. The ensuing neural bursting may accordingly be thought of as the alternation of APs with irregular periods of no activity and explains why the Gaussian distribution of interspike intervals otherwise observed for an autaptic neuron without astrocyte, is instead heavy-tailed in the presence of gliotransmission (Volman et al, 2007).

3.2 Modulation of neural excitability

Two pathways for regulation of neuronal excitability by glia have hitherto been explored by computational studies: one by glia-mediated control of K^+ homeostasis, the other by modulation of excitatory synapses by astrocytes. In the first case, the fact that cortical astrocytes, Müller glia in the retina, or Bergmann glia in the cerebellum, buffer extracellular K^+ redistributing it to sites of lower concentration, locally changes the resting membrane potential of neurons by the **ref.** GOLDMAN-HODGKIN-KATZ EQUATION as well as the Nernst potential of individual ions

(**ref.** NERNST EQUATION), thereby modulating the neuron’s threshold for AP generation. This modulation can be crucial to set the tone of neuronal firing in healthy physiological conditions since blocking glial buffering could turn random firing maintained by random external stimulation into periodic bursting, and eventually lead to permanent spike inactivation (Bazhenov et al, 2004). Mechanistically, glial K^+ buffering can be by different combinations of passive and active transport systems, which, however, share an interplay between glial ATP-driven Na^+/K^+ pumps (NKPs) and Kir channels. Depending on neuronal activity, this interplay can mediate non-trivial positive feedback on neuronal firing, for example, promoting AP generation in conditions of low neuronal firing (Somjen et al, 2008), or turning regular spiking dynamics into bursting (Somjen et al, 2008; Øyehaug et al, 2012; Cui et al, 2018).

Control of neuronal firing by modulation of excitatory synaptic transmission by astrocytes could instead occur, in principle, both by pre- and postsynaptic pathways of gliotransmission, and intrasynaptically, by glutamate uptake by astrocytic transporters. In the first scenario, the rationale for modulation essentially follows that of equations 7–9, where Ca^{2+} -dependent gliotransmission could be triggered either by synaptically-activated astrocytic metabotropic receptors (De Pittà and Brunel, 2016) or by Na^+ influx into the astrocyte by glutamate transporters which in turn regulates Ca^{2+} influx into the astrocyte by Na^+/Ca^{2+} -exchangers (Flanagan et al, 2018), though this latter possibility requires experimental validation. In the second scenario, detailed kinetic models of astrocytic transporters and AMPA and NMDA synaptic receptors suggest instead that control of glutamate clearance by astrocytic transporters could modulate postsynaptic receptors’ activation and desensitization thereby modulating the kinetics of postsynaptic current. This results in subtle changes in spike arrival timings and spike failures that modulate the firing pattern of the postsynaptic neuron (Allam et al, 2012).

3.3 Neuron-glia interactions in neural networks

The importance of uptake of neurotransmitters such as glutamate and GABA by astrocytes in setting the tone of neural network activity has only been partially explored in the framework of **ref.** NEURAL MASS ACTION modeling, yet producing two interesting predictions (Garnier et al, 2016). First is the observation that a deficiency of GABA uptake by astrocytes increases the threshold for neuronal activation in a linear fashion. Second is the prediction that, in the presence of deficient astrocytic glutamate uptake, neural activity may either be reduced or enhanced or may display a transient of high activity before stabilizing around a new regime whose firing frequency is close to the one measured in the absence of astrocyte deficiency. Significantly, the somehow counterintuitive possibility that neural activity could decrease despite extracellular glutamate accumulation due to deficits in astrocytic uptake may be observed only in the presence of sufficient interneuron hyperexcitability.

More generally, in the framework of neuronal network theory, modulation of neuronal excitability and synaptic transmission by glia is expected to modulate the balance of excitation (E) vs. inhibition (I) with the potential to regulate network activity dramatically. This possibility follows by the analysis of the few available neuron-glia network models, which come in different flavors in terms of the combination of different E–I network configurations and different choices of neuronal (and synaptic) models and astrocytic signaling pathways (Savin et al, 2009; Ullah et al, 2009; Volman et al, 2013; Savtchenko and Rusakov, 2014). Nonetheless, all these models eventually envisage an effect of glial signaling in terms of a modulation of synaptic drive, either at excitatory (Savin et al, 2009; Savtchenko and Rusakov, 2014) or excitatory and inhibitory synapses (Ullah et al, 2009; Volman et al, 2013; Garnier et al, 2016), which accounts for the emergence of variegated network activity. With this regard, a model by Ullah et al (2009) considers the effect of astrocytic regulation of extracellular K^+ and Na^+ on firing dynamics of

both excitatory and inhibitory neurons with voltage-dependent synaptic inputs. Accordingly, neuronal membrane potential dynamics depends on K^+ and Na^+ homeostasis regulated by astrocytes, and so does the network’s E–I balance. In this framework, brief (30 ms-long) step increases of E-to-E synaptic strength, which could loosely ensue from glial glutamate exocytosis, promote transient increases of neuronal firing, whose duration, however, depends on extracellular K^+ concentration (Ullah et al, 2009). In particular, for plausible non-pathological values of this concentration, the network could display transient episodes of persistent enhanced firing, which are reminiscent of persistent activity during UP states (Sanchez-Vives and McCormick, 2000; Amzica et al, 2002; McCormick et al, 2003), as well as during delay periods of working memory tasks (Funahashi et al, 1989; Goldman-Rakic, 1995).

Similar observations may also be made by other models which consider different scenarios of gliotransmission, such as short-term modulations of E-to-I synaptic connections by glutamatergic or purinergic gliotransmission (Savtchenko and Rusakov, 2014), or homeostatic upregulation of excitation by glial $TNF\alpha$, although this latter scenario could also account for the emergence of paroxysmal activity in various pathological conditions (Volman et al, 2013). Significantly, these models identify in the spatial extent of gliotransmission a further key factor for the regulation of glia-mediated episodes of increased network activity, ranging from their frequency and duration (Volman et al, 2013) to the degree of network synchronization and the average firing rate of single neurons during their occurrence (Savtchenko and Rusakov, 2014). With this regard, the transient depression of synapses within an astrocytic anatomical domain, which could mimic release-decreasing gliotransmission or temporary disruption of release-increasing gliotransmission, correlates with a decrease of neuronal firing and synchronization, which is more significant for larger astrocytic domains (Savtchenko and Rusakov, 2014).

3.4 Regulation of synaptic transmission and plasticity

Modulation of synaptic release probability by gliotransmitters may occur on multiple time scales (De Pittà et al, 2015). On the one hand, it may last for tens of seconds up to a few minutes, thus affecting synaptic transmission and network computations only temporarily. In this context, theoretical investigations hint that synapses that display short-term depression can turn facilitating, and vice versa, by gliotransmission (De Pittà et al, 2011). At the same time, the filtering characteristic of the synapse for incoming APs also changes based on the history of astrocytic activation (De Pittà, 2019). On the other hand, it is also possible for gliotransmission and its effects on synaptic transmission to last for tens of minutes: that is on time scales that could promote long-term plastic changes of the synapse. In this latter scenario, the change of synaptic weight w_{ij} of a synapse from neuron j to neuron i respectively firing at x_j , x_i , and in the presence of gliotransmitter release at rate γ , may be expressed by $\dot{w}_{ij} = F(w_{ij}; x_i, x_j, \gamma)$, where F is a generic function which we can expand about $x_i = x_j = \gamma = 0$, so that

$$\begin{aligned} \dot{w}_{ij} \approx & c_2^{\text{corr}} x_i x_j + c_2^{\text{pre}} x_i^2 + c_2^{\text{post}} x_j^2 \\ & + c_2^{\text{g-pre}} x_i \gamma + c_2^{\text{g-post}} x_j \gamma + c_2^{\text{glia}} \gamma^2 \\ & + c_1^{\text{pre}} x_i + c_1^{\text{post}} x_j + c_1^{\text{glia}} \gamma + c_0(w_{ij}) + O(x_i, x_j, \gamma) \end{aligned} \quad (10)$$

In the absence of gliotransmission ($c_2^{\text{g-pre}} = c_2^{\text{g-post}} = c_2^{\text{glia}} = c_1^{\text{glia}} = 0$), the above equation results in prototypical **ref. HEBBIAN LEARNING** by $c_2^{\text{corr}} > 0$ (or anti-Hebbian learning for $c_2^{\text{corr}} < 0$) (Gerstner and Kistler, 2002). This however may not be the case in the presence of gliotransmission, insofar as the requirements for associativity encompassed by Hebbian plasticity may not be sufficient to generate a change of synaptic weight. Correlation between pre- and postsynaptic activities reflected by c_2^{corr} in fact, now sums with correlations between these

activities and the effect of gliotransmission on pre- ($c_2^{\text{g-pre}}$) and postsynaptic receptors ($c_2^{\text{g-post}}$) (De Pittà and Brunel, 2016), including additional effects on synaptic weight borne by gliotransmission alone which, for example, could mirror SICs which could be independent of postsynaptic activity (Wade et al, 2011).

Broadly speaking, how modulations of synaptic plasticity by glia could ultimately affect learning remains to be investigated, although few theoretical studies offer some enticing insights into the topic. Porto-Pazos and collaborators investigated performance of an astrocyte-inspired learning rule to train deep networks in data classification (Porto-Pazos et al, 2011; Alvarellos-González et al, 2012; Mesejo et al, 2015). They consider a feedforward network architecture where each neuron in the intermediate (hidden) layers associate with an astrocyte that modulates all the neuron’s outgoing connections. Each astrocyte is described by a quadruple (μ, κ, a, b) and requires μ stimulations by an associated synapse within κ consecutive time steps to get activated. Upon an astrocyte’s activation, the weights of all synapses associated with that astrocyte are increased by a factor a which could mimic either persistent increases of synaptic release by gliotransmission (Perea and Araque, 2007; Navarrete et al, 2012) or LTP following enhanced postsynaptic NMDA receptor activation by astrocytically-released D-serine (Henneberger et al, 2010). Conversely, if a neuron associated with an astrocyte remains inactive μ times within κ time steps, then the weights of its outgoing synapses are decreased by a factor b – a behavior that loosely reflects the termination of the aforementioned gliotransmitter-mediated effects, and accounts, in the long run, for pruning of inactive synapses (Hua and Smith, 2004).

Several variants of the learning rule were tested, mostly dealing with different handling of astrocyte activations by consecutive neuronal firing exceeding μ ; yet, regardless of the details of the learning (training) procedure, the trained neuron-glia networks were able to outperform identical networks without astrocytes in all discrimination tasks taken into account (Porto-Pazos et al, 2011; Alvarellos-González et al, 2012). The training was however successful if potentiation by astrocytes was less than depression by astrocyte inactivity, that is $a < b$ (Alvarellos-González et al, 2012; Mesejo et al, 2015). Because the change in synaptic weight mediated by an astrocyte at a synapse i at time t depends on the synapse’s weight value at the previous update instant $t - 1$, i.e. $\Delta w_i(t) = a \cdot w_i(t - 1)$ for potentiation and $\Delta w_i(t) = b \cdot w_i(t - 1)$ for depression, the $a < b$ condition assures that potentiation and depression do not cancel out at individual synapses, and that depression globally dominates, possibly preventing the network’s runaway by excitation. On the other hand, the fact that $\Delta w_i(t)$ depends on $w_i(t - 1)$, which in turn depends on $w_i(t - 2)$ by $\Delta w_i(t - 1)$ and so on, suggests that the relative contribution of potentiation over depression at any time at a given synapse depends on the history of synaptic updates which, in turn, reflects the history of the associated astrocyte’s activation.

There is circumstantial evidence that astrocytes could modify the threshold for LTD vs. LTP induction, such as in the supraoptic nucleus – where astrocytic coverage of synapse is reduced during lactation (Panatier et al, 2006). In these conditions, stimuli that are expected to induce LTP, elicit LTD instead, possibly for a reduced NMDA receptor activation by lower extracellular concentrations of astrocytic D-serine due to the increased extracellular space. Based on this experimental finding, and the observation that astrocytic D-serine could gate LTD or LTP induction (Zhang et al, 2008; Henneberger et al, 2010), Philips et al (2017) devised a modified version of the BCM rule (Bienenstock et al, 1982; Gerstner and Kistler, 2002) where the threshold rate of postsynaptic firing for induction of LTD vs. LTP varies proportionally with astrocyte activation, and investigated how this rule affects development of orientation preference maps (OPMs) in a self-organizing network model of the primary visual cortex (V1) (Stevens et al, 2013). In their formulation, activation of an astrocyte is computed by the weighted sum of activities of all synapses within the astrocyte’s anatomical domain of radius R , while the

modified BCM rule only applies to excitatory connections, whereas inhibitory connections and excitatory afferents are trained by a classical Hebbian paradigm. This allows choosing the spatial range of inhibitory connections to match short-distance lateral inhibitory connections found in V1 (Kisvárdy et al, 1997), while leaving the spatial range of lateral excitatory connections dependent on astrocytic radii.

This choice not only allows reproducing map orientation experimentally observed in V1, but also reveals that, upon reduction of astrocytic radius, periodicity of OPMs increases while width of individual hypercolumns decreases (Philips et al, 2017). Inasmuch as astrocyte size varies across species (Oberheim et al, 2009; López-Hidalgo et al, 2016), these results predict a causal link between astrocytic radius and different hypercolumn widths observed in different species (Kaschube et al, 2010). On the other hand, the model fails to explain why V1 in rodents displays a typical salt-and-pepper configuration (Ohki et al, 2005), inasmuch as it predicts the emergence of such configuration in the limit of $R \rightarrow 0$, that is in the absence of astrocytes, which is in apparent contradiction with experimental evidence (Schummers et al, 2008; Chen et al, 2012; Perea et al, 2014).

The type of sliding threshold introduced by Philips and co-workers is conceptually different from the one in the original BCM rule (Bienenstock et al, 1982). In this latter, the sliding threshold is a local quantity that depends on the history of the activation of individual post-synaptic neurons. Conversely, by exploiting the concept of “synaptic islands” – namely sets of synapses stimulating and being regulated by the same astrocyte (Halassa et al, 2007) – Philips and colleagues *de facto* consider a “global” threshold that modulates weight of many synapses in parallel, based on the integral of their activation by their associated astrocyte. In this way, it is as if each astrocyte in Philips et al’s model supervised the signal inducing plastic changes (i.e., the “teaching signal”) throughout the whole synaptic territory defined by its anatomical radius.

The emerging view of Ca^{2+} compartmentation in astrocytes (Bazargani and Attwell, 2016) suggests that, if Ca^{2+} is the mediator of gliotransmission (Sahlender et al, 2014), then its “globality” could be non-trivially defined, as it would likely depend, from time to time, on dynamics of Ca^{2+} microdomains, rather than be solely defined by the astrocyte radius (Volterra et al, 2014). On the other hand, insofar as the criteria for globality are met, we shall note that the underpinning Ca^{2+} signal could be generated either by postsynaptically released endocannabinoids (Navarrete et al, 2014) or by different presynaptic pathways that are related to presynaptic neuronal firing. These presynaptic pathways could include the spillover of synaptically-released neurotransmitters from the synaptic cleft (Araque et al, 2014), as well as other Ca^{2+} pathways linked with extracellular ion homeostasis (Figure 1). Remarkably, if we consider this second option – namely that the global Ca^{2+} -dependent, gliotransmitter-mediated teaching signal carries information about the activity of presynaptic neurons –, it is possible to envisage a biologically plausible learning rule to learn precise spike patterns and reproduce them precisely and robustly over trials. This argument was elegantly demonstrated by Brea, Senn, and Pfister (2013) in recurrent networks where neurons were arbitrarily separated between visible vs. hidden ones. In those networks, teaching to and accurate recall from visible neurons of an arbitrary spiking sequence is possible devising a learning rule that minimizes the Kullback-Leibler divergence of the spiking distribution produced by the network from the target distribution (i.e., the sequence to be learned). Such learning rule also discriminates between visible and hidden neurons and specifically modulates those synapses onto hidden neurons based on a threshold for LTD vs. LTP that is updated at each time step to account for the global activity of visible neurons. As the same authors argue that astrocytes could mediate this threshold, they also note that for this possibility to be realistic, astrocytes “need to know” which neurons are visible and which are hidden – a scenario that could be brought forth by a combination of the reciprocal

arrangement between astrocytes and neuronal and vascular structures, and the chemical signals between them yet to be identified.

3.5 Glial cytokine signaling

There is emerging evidence that, apart from macroglia, microglia, too, could be involved in the genesis and function of neural circuits in the healthy brain (Kettenmann et al, 2013). This possibility is further supported by the growing recognition that molecules like proinflammatory cytokines such as $\text{TNF}\alpha$, which are generally associated with the microglial immunocompetent response, but could also be released from astrocytes (Bezzi et al, 2001), may be found in healthy, non-inflamed brain tissue, possibly with a signaling role other than proinflammatory (Wu et al, 2015). Significantly, microglial could control extracellular $\text{TNF}\alpha$ in a bimodal fashion, first increasing it up to a peak concentration, and then recovering its constitutive extracellular concentration (Chao et al, 1995). Because at constitutive concentrations of $<300\text{ pM}$, $\text{TNF}\alpha$ seems necessary for glutamatergic gliotransmission, but above those concentrations, it could promote neurotoxicity (Santello and Volterra, 2012), modeling of **ref.** CYTOKINE NETWORKS, MICROGLIA AND INFLAMMATION may be used to identify critical macro- and microglial pathways underpinning this dual signaling role by $\text{TNF}\alpha$. In this context, variance-based global sensitivity analysis of a microglial cytokine signaling network identifies two further cytokines – IL-10 and $\text{TGF}\beta$ – as possible key regulators of microglial $\text{TNF}\alpha$. Both those molecules are promoted by $\text{TNF}\alpha$ while exerting negative feedback on it. However, because the kinetics of IL-10-mediated feedback is faster than that by $\text{TGF}\beta$, they can end up exerting opposing effects on extracellular $\text{TNF}\alpha$, depending on temporal differences in their expression: reduction of $\text{TNF}\alpha$ peak concentration by IL-10 may indeed be counteracted by the ensuing reduction of $\text{TGF}\beta$ production with the potential to turn the traditionally anti-inflammatory action of these cytokines, proinflammatory instead (Anderson et al, 2015).

The study of $\text{TNF}\alpha$ signaling, possibly of (micro)glial origin, is also linked with homeostatic mechanisms of synaptic plasticity (Steinmetz and Turrigiano, 2010). A case study is the mechanism of ocular dominance plasticity (ODP) whereby monocular deprivation (MD), during a critical period of development, causes a rearrangement of neuronal firing properties in the binocular visual cortex. In this fashion, cells that are initially biased to respond to inputs from the closed eye, end up responding more strongly to inputs from the open eye (Wiesel, 1982). As revealed by experiments in the visual cortex of juvenile mice, MD-triggered ODP results from two separable plastic processes: (i) a rapid, Hebbian-like LTD, that is responsible for weakening the closed eye’s response within the first three days of MD; and (ii) a slow homeostatic response where $\text{TNF}\alpha$ – possibly of glial origin – scales up excitatory synapses and strengthens the open eye’s response approximately by the third day of MD (Kaneko et al, 2008). Because of the large separation between time scales of Hebbian vs. homeostatic plasticity, conventional models of synaptic plasticity where Hebbian and homeostatic plasticity are assumed to compete to set synaptic strength, cannot account for MD-induced ODP. In those models, in fact, a small perturbation of synaptic strength away from equilibrium is promptly amplified by the fast positive feedback of Hebbian plasticity, and this amplification can hardly be prevented by the slow homeostatic feedback, making the network prone to instability (Toyoizumi et al, 2014; Zenke et al, 2017). To avoid this scenario, an adequate description of MD-induced ODP should leverage instead on the consideration that observed Hebbian LTD and glial homeostatic scaling are independent of each other during MD (Kaneko et al, 2008) so that they both must separately reach their own stable state for the network to be stable. This could, in principle, be accounted for by the fact that plastic changes induced both by Hebbian learning and by homeostatic scaling can saturate to minimal and maximal values, making these two plasticity mechanisms

inherently stable (Beattie et al, 2002; O’Connor et al, 2005). However, in practice, at least two further conditions must be met to be able to reproduce ODP robustly (Toyoizumi et al, 2014). First, homeostatic plasticity must also scale minimum and maximum values of synaptic strength attained by mere Hebbian learning. Second, homeostatic scaling must depend on instantaneous neuronal activity, like postsynaptic depolarization, since this latter correlates with extracellular glutamate levels, which, in turn, regulate the glial release of TNF α (Bezzi et al, 2001; Stellwagen and Malenka, 2006). Based on these arguments then, it is possible to devise a working model of MD-induced plasticity where synaptic strength w can be recast as the product of two factors: a synapse-nonspecific factor H , applicable to the whole postsynaptic cell and controlled by slow glial TNF α -mediated homeostatic scaling, and a synapse-specific factor ρ regulated by fast Hebbian plasticity, i.e., $w = H \cdot \rho$ (Toyoizumi et al, 2014). This description of synaptic strength then accounts for the intriguing possibility that slow glial TNF α signaling in the visual cortex could intrinsically balance with fast Hebbian plasticity by instantaneously rescaling the range of synaptic strength values attained by Hebbian learning. The multiplicative scaling envisaged by the expression for w is critical for glial homeostasis to maintain the relative strength between different synapses. Moreover, because it also affects minimal and maximal synaptic weights, it can thereby bring the network’s activity level toward equilibrium without disturbing the intrinsic stability of the Hebbian dynamics and without being overwritten by this latter. In parallel, the presumed instantaneous dependence of H on (post)synaptic activity guarantees network stability making glial homeostasis able to readily follow perturbations of the network’s activity caused by fast Hebbian learning (Toyoizumi et al, 2014).

4 Temporal and spatial scales of neuron-glia interactions

4.1 Morphology and structural plasticity

The large heterogeneity of glial cells, even within individual types such as oligodendrocytes, microglia, and astrocytes, makes the notion of average cell anatomy of little significance. The number of axons myelinated by single oligodendrocytes, for example, considerably changes with axon caliber, and so does the degree of myelination in terms of internodal lengths, ultimately dictating different conduction speeds. Oligodendrocytes are generally classified into four types, depending on the caliber of the axons they myelinate, with the possibility for intermediate types to exist too. Accordingly, types I/II are found in association with small ($<4\ \mu\text{m}$) axons, whereas types III/IV myelinate larger axons. The morphological values provided in Table 1 are from Butt (2013).

More complicated is the description of microglia since, in the healthy brain, these cells display a ramified morphology whose processes continuously extend and retract at rates of 0.4–3.8 $\mu\text{m}/\text{min}$ (Nimmerjahn et al, 2005). The classical study by Lawson et al (1990) arguably still provides the most comprehensive characterization of microglia anatomy and distribution in the brain uptodate. Accordingly, microglia were shown to be present in large numbers in all major divisions of the brain but not to be uniformly distributed. There is, in fact, a more than five-fold variation in the density of microglial processes between different regions, with higher density in the hippocampus, average one in the cortex and hypothalamus, and lower one in the cerebellum. Overall, microglia surface density ranges between $\sim 50 - 140\ \text{cells}/\text{mm}^2$, with individual cells displaying a large variability in surface area, from $<200\ \mu\text{m}^2$ in the cortex to $>500\ \mu\text{m}^2$ in the hippocampal formation, which likely associates with variegated morphological complexity, as reflected by a perimeter-to-convex perimeter ratio of 5 for cortical microglia but >8 for microglia in the hippocampus. Volumetric data on microglia is not yet available.

Protoplasmic astrocytes represent the main astrocyte type in the gray matter and appear to

be among the most structurally intricate cells of the brain (Reichenbach and Wolburg, 2013). They display a highly branched morphology with some degree of polarization that is probably region-specific (Chao et al, 2002). At least one of the cell branches (or “processes”) is bearing one or several perivascular endfeet such that the surfaces of the blood vessels in the CNS are virtually completely ensheathed by astrocytic endfoot plates (Mathiisen et al, 2010). Astrocyte volume in rodents has been reported to range from 14700–22 906 μm^3 in the cortex to 65900–85 300 μm^3 in the hippocampus (Bushong et al, 2002; Ogata and Kosaka, 2002; Chvátal et al, 2007; Halassa et al, 2007). These figures, however, are not indicative of the morphological complexity of these cells, as mirrored instead by a large surface-area-to-volume ratio in the range of 18.9–33.0 μm^{-1} (Hama et al, 2004). Single anatomical domains of cortical astrocytes were reported to include from 4 to 8 neuronal somata (Halassa et al, 2007). A direct measure of the number of synapses within an astrocytic domain instead is not available but can be estimated from synaptic densities. With this regard considering an average of 0.89 synapse/ μm^3 in the cortex (Kasthuri et al, 2015) and 2.13 synapse/ μm^3 in the hippocampus (Kirov et al, 1999), we get figures for the number of synapses within the above astrocytic volumes that equal to \sim 13000–20400 synapses/astrocyte in the cortex and \sim 140000–182000 synapses/astrocyte in the hippocampus.

It is not clear to what extent the number of synapses ensheathed by astrocytes could change during activity by structural plasticity of perisynaptic astrocytic processes (Haber et al, 2006), and cell swelling (Florence et al, 2012), but, likely, the functional interactions between astrocytic and synaptic elements do so. Typical rate values for changes of cell morphology and ECS shrinkage ensuing from astrocytic swelling can then be estimated by experimental observations that directly link these changes with (putative) functionally relevant levels of neuronal activity. With this regard, perisynaptic astrocytic processes undergo multiple retractions and protrusions of $>5 \mu\text{m}$ length in correlation with neuronal activation (Haber et al, 2006), and LTP induction correlates with an average remodelling rate of $<40 \text{ nm/s}$ in hippocampal astrocytic processes (Perez-Alvarez et al, 2014). Putative physiological HCO_3^- increases in the ECS trigger astrocytic swelling, which can be quantified in terms of percentage variation of the cell’s surface area to baseline HCO_3^- concentrations. This swelling can be well described by a monoexponential curve of the type $\Delta_{\text{max}}(1 - \exp(-rt))$ with $r = 0.08 \text{ s}^{-1}$, $\Delta_{\text{max}} \approx 20\%$, resulting in an initial linear rate of surface area increase of $\sim 1.5 \Delta\%/s$ ($\Delta\%/s$: percentage variation in the unit time) (Florence et al, 2012). Alternatively, ECS shrinkage possibly related to astrocyte swelling appears to increase linearly with duration of stimulation by rates in between $\sim 0.3\text{--}0.7 \Delta\%/s$, and recover to original volumes upon cessation of stimulation with decay times $>10 \text{ s}$ (Larsen et al, 2014).

4.2 Calcium signaling

Study of Ca^{2+} signaling in microglia and oligodendrocytes is still in its infancy and the only estimates of rise (τ_r), decay times (τ_d), and full width at half maximum (FWHM) of this signaling pathway may be derived from purinergically-evoked Ca^{2+} elevations in microglia *in vivo* (Brawek et al, 2017; Brawek and Garaschuk, 2017) and oligodendrocyte *in situ* (James and Butt, 2001). Time constant are estimated by fitting experimental Ca^{2+} traces ($c(t)$) by a difference of two exponential, i.e. $c(t) = C (\exp(-t/\tau_d) - \exp(-t/\tau_r))$ where C is a normalization factor equal to $C = (T^{\frac{\tau_x}{\tau_d}} - T^{\frac{\tau_x}{\tau_r}})^{-1}$ with $T = \tau_r/\tau_d$ and $\tau_x = \tau_r\tau_d/(\tau_d - \tau_r)$. Accordingly, for oligodendrocytes (based on $n = 20$ Ca^{2+} traces): $\tau_r = 6.5 \pm 1.2 \text{ s}$, $\tau_d = 6.7 \pm 1.1 \text{ s}$ and FWHM = $14.2 \pm 2.6 \text{ s}$; and for microglia ($n = 6$): $\tau_r = 0.8 \pm 0.3 \text{ s}$, $\tau_d = 5.0 \pm 0.1 \text{ s}$ and FWHM = $3.9 \pm 1.3 \text{ s}$.

The vast majority of observations on glial Ca^{2+} signaling has been made so far on astrocytes, although several aspects of this signaling remain to be investigated and cannot be challenged

by present techniques (Rusakov, 2015). For example, it is not yet possible to resolve Ca^{2+} signals in fine perisynaptic astrocytic processes (e.g., lamellae or filopodia), although we are now in the conditions of resolving Ca^{2+} dynamics in the three-dimensional space (Bindocci et al, 2017). Generally speaking, when considering astrocytic Ca^{2+} signals *in vivo*, different factors beyond development and technical approaches must be taken into account, such as whether these signals were recorded in awake or asleep/anesthetized animals, what brain area they occurred in, if they are spontaneous or evoked by stimulation, and in this latter case, what stimulus protocol was adopted (Rusakov, 2015). In what follows, we only consider estimates for protoplasmic astrocytes, which constitute the main astrocyte type of the rodent’s grey matter. The reader should keep in mind that Ca^{2+} dynamics in other astrocyte types as well as in Müller cells and Bergmann glia could be different (Matyash and Kettenmann, 2010).

In astrocytes, spontaneous somatic/whole cell Ca^{2+} signals are rare ($\nu \approx 5.8\text{--}9.2$ mHz), and characterized by a rise time in the range of $\tau_r \approx 2\text{--}20$ s, a decay time $\tau_d \approx 3\text{--}25$ s, and a full width at half maximum FWHM $\approx 5\text{--}160$ s (Hirase et al, 2004; Nimmerjahn et al, 2004; Wang et al, 2006; Bindocci et al, 2017). Recent estimates of these quantities in microdomains of astrocytic processes and endfeet provide: $\nu \approx 6\text{--}8$ mHz, $\tau_r < 0.7\text{--}5$ s, $\tau_d < 6\text{--}10$ s, FWHM $\approx 0.35\text{--}3$ s in processes, and $\nu \approx 29\text{--}40$ mHz, $\tau_r < 3\text{--}18$ s, $\tau_d < 2\text{--}30$ s, FWHM $\approx 0.75\text{--}12$ s at endfeet (Bindocci et al, 2017). The onset delay of these events can be remarkably short and follow neuronal stimulation within $<0.3\text{--}3$ s (Winship et al, 2007; Bindocci et al, 2017; Stobart et al, 2018). Significantly, there appears to exist a clear distinction in distribution of values of ν , τ_r and τ_d with respect to Ca^{2+} events whose FWHM is below vs. above ~ 1.5 s (Bindocci et al, 2017). Furthermore size of Ca^{2+} microdomains in processes appears slightly larger during stimulation with respect to resting state, i.e. $60.7 \pm 24.3 \mu\text{m}^3$ vs. $40.50 \pm 3.11 \mu\text{m}^3$, whereas a large dynamical richness of Ca^{2+} events is reported at the somatic level, with average signaling volumes of the order of $4470 \pm 1051 \mu\text{m}^3$, with largest events being in the order of $6375 \pm 1106 \mu\text{m}^3$ (estimated range of $\sim 890\text{--}10\,000 \mu\text{m}^3$) (Bindocci et al, 2017). Intracellular Ca^{2+} propagation may be estimated in the range of $\sim 16 \pm 8 \mu\text{m/s}$ (Di Castro et al, 2011, Supplementary Figure 5), whereas speed of intercellular Ca^{2+} waves, measured mostly in brain slices so far, is in the range of $\sim 8\text{--}20 \mu\text{m/s}$ (Scemes and Giaume, 2006; Oberheim et al, 2009), although a recent study *in vivo* reported on large Ca^{2+} waves that could recruit >80 astrocytes, and propagate as fast as $61 \pm 22 \mu\text{m/s}$ (Kuga et al, 2011).

4.3 Glutamate-glutamine cycle and astrocyte-to-neuron lactate shuttle

Both GGC and ANLS rely on glutamate (and GABA) uptake by astrocytic transporters. The transporter currents for these two neurotransmitters recorded in hippocampal astrocytes display a marked time scale separation. In the adult mice, the 20%–80% time rise of astrocytic glutamate uptake was estimated in the range of 0.92–1.65 ms (Diamond, 2005) although some investigators suggest that a longer 10%–90% rise time, up to 5.98 ± 0.38 ms, could also be reached (Kinney and Spain, 2002). Decay times are instead reported in the range of 4.64–5.43 ms. GABA uptake is substantially slower with 10%–90% rise and decay time constants comprised between $>410.5\text{--}543.83$ ms and $>0.93\text{--}4.34$ s, respectively (Kinney and Spain, 2002). A further limiting factor of GGC and ANLS is substrate availability, for which little is known *in vivo* so far. Nuclear magnetic resonance data in anesthetized rats suggest a rate of glutamine synthesis by astrocytes between $\sim 0.13\text{--}0.21 \mu\text{mol}/\text{min} \cdot \text{g}$, which is nearly half of the estimated consumption rate of glutamate by Krebs cycle, thus hinting glutamine synthesis as a major metabolic pathway in the rat cortex (Sibson et al, 1997; Rothman et al, 2003). For lactate production by individual astrocytes, astrocytic intracellular NADPH signaling in response to synaptically-activated metabotropic glutamate receptors (mGluRs) can be adopted as the read-

out of different scenarios of neuronal activity and brain states in conditions of simulated hyperemia (high pO_2) or vasoconstriction (low pO_2) (Gordon et al, 2008). This is because the enzyme that is responsible of lactate synthesis – i.e., lactate hydrogenase – is NADPH-dependent (Figure 1, *purple pathway*) so that increases and decreases of NADPH following mGluR-mediated astrocytic activation can directly be linked to intracellular lactate metabolism by astrocytes, resulting in estimates for rise and decay time constants for this latter in between 4.1–5.2 s, with lower values associated with high pO_2 and vasoconstriction (Gordon et al, 2008).

4.4 Gliotransmission

Estimates of time scales of modulation by gliotransmitters should be based on experimental data (mostly *in situ*) that provide information on the time evolution of the effect of gliotransmission on synaptic transmission. Table 1 includes such estimates for short- and long-term effects of release-increasing glutamatergic gliotransmission, and short-term, release-decreasing purinergic gliotransmission (Perea and Araque, 2007; Covelo and Araque, 2018). A biexponential function (Section 4.2) can be used to fit time series data of synaptic release probability ($p(t)$) following astrocytic Ca^{2+} activation (set at $t = 0$), thereby obtaining: for glutamatergic gliotransmission $\tau_r > 0.05 - 0.2$ s, $\tau_d = 5.9 - 6.7$ s ($n = 2$, short-term); $\tau_r = 6.2 - 28.3$ s, $\tau_d = 18.7 - 95.7$ s ($n = 3$, long-term); for purinergic gliotransmission ($n = 2$): $\tau_r = 1.6 - 8.2$ s, $\tau_d = 8.2 - 12.0$ s. It is also possible to estimate the rate of D-serine-dependent synaptic potentiation in terms of percentage variation of synaptic strength in the unit time, under the assumption of a linear increase of synaptic strength in the presence of activity-dependent D-serine release from astrocytes. The range of values for this postsynaptic pathway of gliotransmission provided in Table 1 was estimated from Yang et al (2003) and Takata et al (2011).

Concerning regulation of AMPA and GABA_A receptors by glial TNF α (Stellwagen and Malenka, 2006), The average rate of change for expression of postsynaptic AMPA and GABA_A receptors by glial TNF α (Stellwagen and Malenka, 2006) may be derived from the ratio between the total percentage change or receptor expression with respect to control ($\Delta\%$) over the duration of TNF α stimulus (T_α). In this fashion, for hippocampal receptors: 157% \pm 15% increase of AMPA receptors, and 12% \pm 4% decrease of GABA_A receptors were reported for TNF α applications of $T_\alpha = 15 - 25$ min (Stellwagen et al, 2005), whereas a decrease of 25% – 30% of GABA_A receptors was measured for $T_\alpha = 45$ min (Pribrag and Stellwagen, 2013). These data translate into rate values of $\sim 5-12$ $\Delta\%/min$ and $\sim -0.3-0.7$ $\Delta\%/min$, respectively for AMPA and GABA_A changes. One should however keep in mind that the effect of TNF α is region and/or cell-specific, insofar as the AMPA-to-NMDA ratio was shown to increase from 1.75 to 3 in hippocampal pyramidal cells in the presence of TNF α ($T_\alpha = 1 - 2$ h), but to decrease from 3.7 to 2.5 at medium spiny neurons in the striatum (Lewitus et al, 2014).

4.5 Ion homeostasis

Extracellular ion homeostasis depends on the brain region and evolves with ongoing neuronal activity. At the rat’s optic nerve, glia K^+ buffering displays a typical bi-exponential behavior, with a rise time that may slightly increase from ~ 0.83 s to ~ 1.6 s as a 10 Hz stimulus is delivered either for 1 s or 10 s (Ransom et al, 2000). Buffering time by re-equilibration of extracellular K^+ concentration, mostly by inward-rectifying K^+ channels in combination with NKPs, is typically large, being comprised between 3.9 ± 1 s and 18 ± 0.6 s (Ransom et al, 2000; D’Ambrosio et al, 2002; Chever et al, 2010). Significantly, this buffering time may considerably shorten in the presence of glial Ca^{2+} signaling, and thereby modulations of glial NKPs, with both rise and decay time of extracellular K^+ converging to $\sim 0.9-5.0$ s (Wang et al, 2012b,a). There is little information on the spatial extent of glia-mediated K^+ buffering *in vivo*, although intracellular

recordings in glia pairs in the suprasylvian gyrus suggest that it is probably fast, with propagation speeds $>30\ \mu\text{m}/\text{second}$ (Amzica et al, 2002). Intriguingly, intracellular Na^+ propagation in hippocampal astrocytes (although demonstrated so far *in situ*) could be at least two-fold faster, but decay to $2\text{--}10\ \mu\text{m}/\text{s}$ for intracellular glial sites $>60\ \mu\text{m}$ far from the stimulus locus (Langer et al, 2012).

4.6 Regulation of the blood flow

Ca^{2+} -dependent regulation of blood flow by astrocytes is dependent on brain state, possibly with vasoconstriction observed in the presence of hyperemia, and vasodilation in association with hypoemia (Gordon et al, 2008). The onset of astrocyte-mediated dilations or constrictions in different brain areas, generally occur within $<1\text{--}3\text{s}$ from the start of astrocytic Ca^{2+} signaling (Zonta et al, 2003; Mulligan and MacVicar, 2004; Otsu et al, 2015). On the other hand, astrocytes seem to promote vasoconstriction to a larger magnitude than vasodilation, since reported percentage decreases of blood vessel diameters mediated by astrocytes could be $>20\%$, whereas observed increases are generally $<10\%$ (Zonta et al, 2003; Mulligan and MacVicar, 2004; Gordon et al, 2008). This is mirrored by linear rates of percentage vessel diameter variation that range between $1.6\text{--}1.7\ \Delta\%/s$ for vasoconstriction (Mulligan and MacVicar, 2004) but only between $>0.05\text{--}0.3\ \Delta\%/s$ for vasodilation (Zonta et al, 2003). Significantly, these figures depend on the number of astrocytic endfeet simultaneously activated on the same blood vessel, since, for example, a single endfoot could trigger a $9.1 \pm 0.7\%$ vasoconstriction, but multiple endfeet could account for a three-fold larger reduction of vessel diameter (Mulligan and MacVicar, 2004).

5 Conclusion

Modeling of neuron-glia interactions is an emerging field of Computational Neuroscience. The ubiquity of these interactions and the possibility that they may occur within the time and spatial scales that are usually ascribed to neuronal and synaptic function, calls for a revision of current neuron-based modeling paradigms to include potentially relevant effects mediated by glial cells. The modeling arguments discussed in this chapter go in such direction, further hinting a fundamental design of neuronal circuits where their structure and function are possibly intertwined with that of glia, thereby challenging the traditional Neuron Paradigm of the brain, in favor of an extended, more realistic Neuron-Glia one.

6 Acknowledgments

Writing of this chapter was made possible by the generous support of the Junior Leader Fellowship Program by “la Caixa” Banking Foundation (LCF/BQ/LI18/11630006), as well as by the support of the Basque Government through the BERC 2018-2012 program, and by the Spanish Ministry of Science, Innovation and Universities: BCAM Severo Ochoa Accreditation SEV-2017-0718.

7 Cross-references

ref. BRAIN ENERGY METABOLISM

ref. CALCIUM-DEPENDENT EXOCYTOSIS, BIOPHYSICAL MODELS

ref. CYTOKINE NETWORKS, MICROGLIA AND INFLAMMATION

ref. COMPUTATIONAL MODELING OF INTRACELLULAR ASTROCYTE Ca^{2+} SIGNALS

ref. GOLDMAN-HODGKIN-KATZ EQUATION
ref. HEBBIAN LEARNING
ref. NERNST EQUATION
ref. NEURAL MASS ACTION
ref. SHORT TERM PLASTICITY, BIOPHYSICAL MODELS

Figure captions

Figure 1. Common interactions between astrocytes and glutamatergic synapses. *Yellow pathway:* astrocytic calcium signaling; *red pathway:* gliotransmission (both glutamatergic and purinergic); *green pathway:* cytokine (TNF α) signaling; *turquoise pathway:* glutamate-glutamine cycle; *blue pathway:* K⁺ buffering; purple pathway: astrocyte-to-neuron lactate shuttle; *brown pathway:* pH buffering; *orange pathway:* glutathione metabolism; *brown pathway:* ascorbic acid exchange; *magenta pathway:* vascular coupling. Modified from De Pittà and Berry (2019b). (---) \rightarrow : (indirectly) promoting pathway; \dashv : inhibiting pathway. 20-HETE: 2-hydroxy-eicosatetraenoic acid; AA: arachidonic acid; Ado: adenosine; AMPA: α -amino-3-hydroxy-5-methyl-4-isoxazolepropionic acid; ADP (ATP): adenosine diphosphate (triphosphate); AQP4: aquaporin channel type 4; ApN: ectoaminopeptidase N; ASC: ascorbic acid (reduced vitamin C) Best-1: bestrophin-1 ion channel; CA: carbonic anhydrase; CIBX: Cl⁻/HCO₃⁻ exchanger; ClC: chloride channel; Cys: cysteine; CysGly: cysteinylglycine; DHA: dehydroascorbic acid (oxidized vitamin C); EAAT: excitatory amino acid transporter; EETs: epoxyeicosatrienoic acids; ER: endoplasmic reticulum; GABA: γ -Aminobutyric acid; GAT: GABA transporter; GDOR: glutathione-dependent dehydroascorbate reductase; GGS/PTG: glycogen synthase/UTP-glycogen-phosphate uridylyltransferase; GJC: gap junction channel; Glu: glutamate; glucose-6P: glucose 6-phosphate; GLUT: glucose transporter; Gly: glycine; GPhos: glycogen phosphorylase; GR: glutathione reductase; GS: glutamine synthetase; GSH: glutathione (reduced form); GSSG: glutathione (oxidized form); γ GT: γ -glutamyl transpeptidase; IP₃: inositol 1,4,5-trisphosphate; iRCs: ionotropic receptor channels; Kir: inwardly rectifying K⁺ channel; Lac: lactate; LDH: lactate dehydrogenase; MCT: monocarboxylate transporter; mGluR: metabotropic glutamate receptor; NAD⁺ (NADH): oxidized (reduced) nicotinamide adenine dinucleotide; NADP⁺ (NADPH): oxidized (reduced) nicotinamide adenine dinucleotide phosphate; NBC: Na⁺-coupled bicarbonate transporter; NCX: Na⁺/Ca²⁺ exchanger; NH₃: ammonia; NHX: Na⁺/H⁺ exchanger; NKCC: Na⁺-K⁺-Cl⁻ co-transporter; NKP: Na⁺/K⁺-ATPase pump; NMDA: N-Methyl-D-aspartate; P₂Y₁: metabotropic purinergic receptor; PAG: glutaminase; PGs: prostaglandins; PLA₂: phospholipase A₂; PPCs: purine-permeable ion channels; Pyr: pyruvate; SACIC: swell-activated chloride channel; SERCA: (sarco)endoplasmic reticulum Ca²⁺-ATPase; SNAT: Na⁺-coupled neutral amino acid transporter; SVCT2: Na⁺-dependent vitamin C transporter 2; TACE: TNF α -converting enzyme; TNF α (TNFR): tumor necrosis factor alpha (receptor); TRPA: transient receptor potential channel; VGCC: voltage-gated Ca²⁺ channel; VGKC: voltage-gated K⁺ channel; VGNC: voltage-gated Na⁺ channel.

Figure 2. Feedback and feedforward pathways in neuron-glia interactions. **A** Presynaptic pathway of gliotransmission stimulated by presynaptically-released neurotransmitters; **B** postsynaptic pathway of gliotransmission stimulated by presynaptically-released neurotransmitters; **C** presynaptic pathway of gliotransmission triggered by postsynaptic endocannabinoid release; **D** postsynaptic pathway of gliotransmission mediated by postsynaptic endocannabinoid release; **E** modulation of glutamatergic gliotransmission by TNF α . **F** K⁺ buffering and regulation of neuronal activity; **G** glutamate-glutamine cycle (GCC); **H** astrocyte-to-neuron lactate shuttle (ANLS); **I** extracellular pH homeostasis; **J** glutathione synthesis; **K** neurovascular coupling; **L** glia-mediated regulation of action potential conduction. [Ca²⁺]_i: intracellular (cytosolic) calcium concentration; [Cys]_i ([Gln]_i): intracellular cysteine (glutamine) concentration; [ECB]_e ([TNF α]_e): extracellular endocannabinoid (TNF α) concentration; [K⁺]_e ([H⁺]_e): extracellular K⁺ (H⁺) concentration; [Nt]_e ([Glu]_e): extracellular neurotransmitter (glutamate) concentration; v_m : membrane potential; AP: action potential; LPS: lipopolysaccharide; SDF1 α : stromal cell-derived factor 1 alpha.

Figures

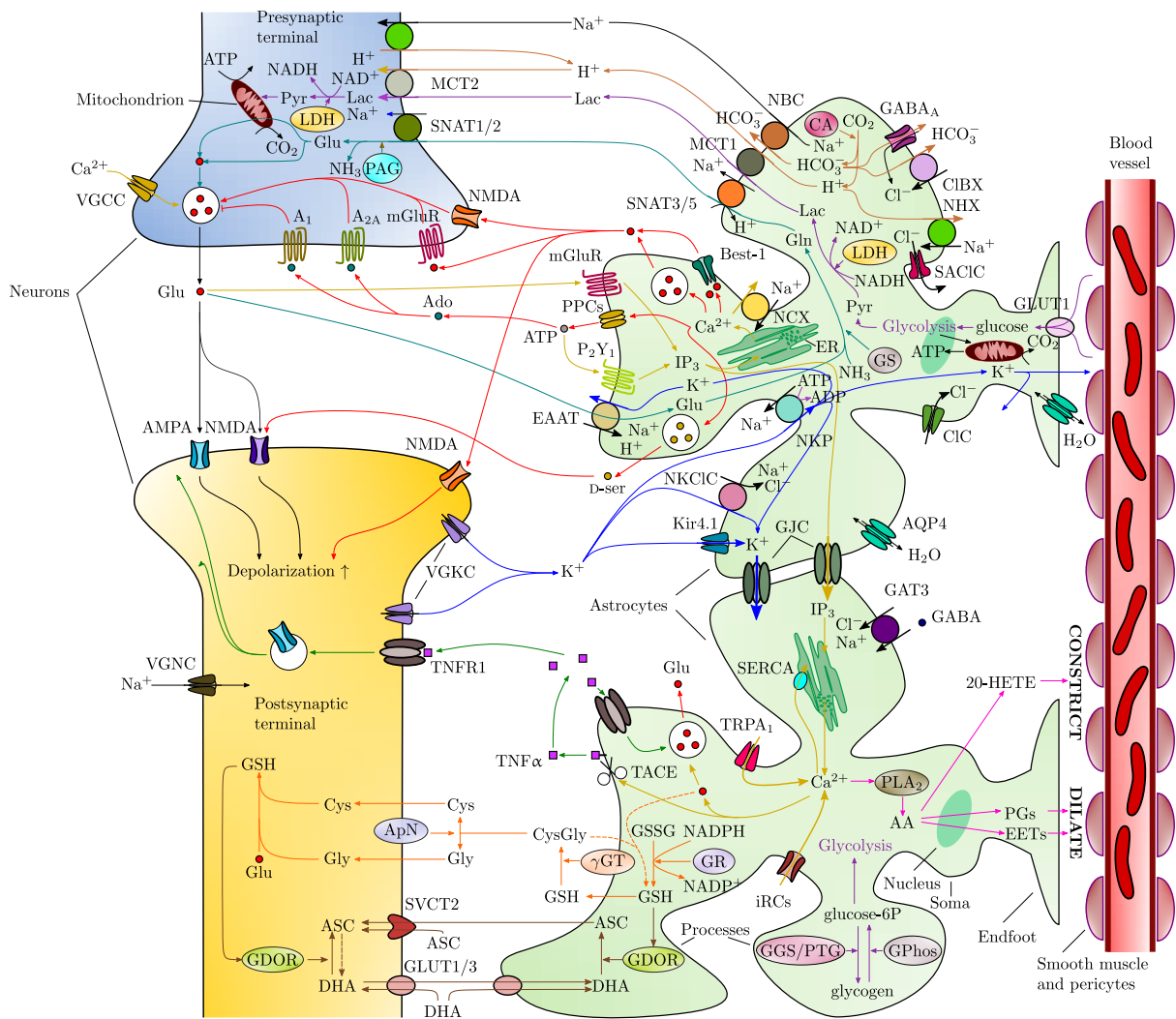


Figure 1. Common interactions between astrocytes and glutamatergic synapses.

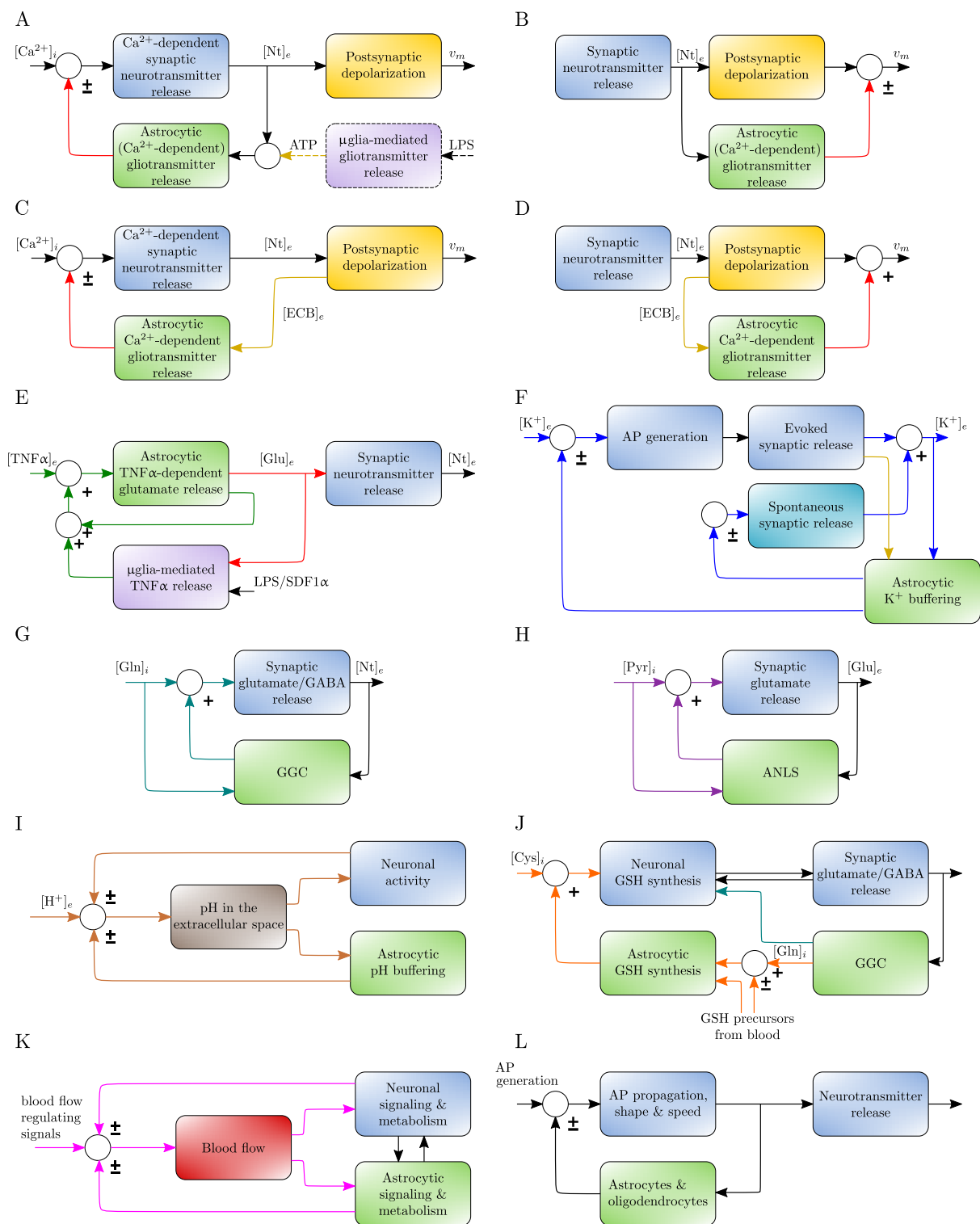


Figure 2. Feedback and feedforward pathways in neuron-glia interactions.

Tables

Table 1. Some relevant spatial and temporal scales of glial signaling in the murine brain.

Description	Range	Units
<i>Morphological features</i>		
Oligodendrocytes (type I/II)		
Associated fiber diameter	<4	μm
Number of myelinated axons per cell	10–50	–
Internodal length	\sim 10–350	μm
Associated axonal conduction speed	<20	$\mu\text{m/s}$
Oligodendrocytes (type III/IV)		
Associated fiber diameter	>4	μm
Number of myelinated axons per cell	1–10	–
Internodal length	\sim 400–1000	μm
Associated axonal conduction speed	80–120	$\mu\text{m/s}$
Microglia		
Surface density	50–140	cells/ mm^2
Surface area	>200–500	μm^2
Perimeter-to-convex perimeter ratio	>5–8	–
Astrocytes (protoplasmic type)		
Cell volume	14700–85300	μm^3
Surface area-to-Volume ratio	18.9–33	μm^{-1}
Neurons per cell	4–8	–
Synapses per cell	13000–182000	–
<i>Structural plasticity</i>		
Process motility		
Astrocytes	<40	nm/s
Microglia	0.4–3.6	$\mu\text{m}/\text{min}$
Astrocytic swelling		
HCO_3^- -mediated percentage cell surface area increase	<1.5	$\Delta\%/s$
Activity-dependent associated ECS shrinkage	<0.3–0.7	$\Delta\%/s$
ECS volume recovery time	>10	s
<i>Non-astrocytic Ca^{2+} signaling</i>		
Oligodendrocytes (soma)		
Rise time	5.2–7.7	s
Decay time	5.5–7.8	s
FWHM	11.6–16.8	s
Microglia (soma)		
Rise time	0.5–1.1	s
Decay time	4.9–5.1	s
FWHM	2.6–5.2	s
<i>Astrocytic Ca^{2+} signaling</i>		
Soma		
Frequency	5.8–9.2	mHz
Rise time	2–20	s
Decay time	3–25	s

continued on the next page

Table 1. *continued*

Description	Range	Units
FWHM	5–160	s
Processes		
Frequency	6–8	mHz
Rise time	<0.2–5	s
Decay time	6–10	s
FWHM	0.35–3	s
Endfeet		
Frequency	29–40	mHz
Rise time	3–18	s
Decay time	2–30	s
FWHM	0.75–12	s
Onset delay (from stimulation)	<0.3–3	s
Microdomain volume		
Soma	~890–10000	μm^3
Processes	~37–85	μm^3
Propagation		
Intracellular speed	~8–24	$\mu\text{m/s}$
Intercellular speed	~8–80	$\mu\text{m/s}$
<i>GGC and ANLS</i>		
Glutamate uptake		
Rise time	0.9–6	ms
Decay time	4.6–5.4	ms
GABA uptake rate		
Rise time	410–544	ms
Decay time	0.9–4.3	s
Glutamine synthesis	0.13–0.21	$\mu\text{mol/min}$
Lactate metabolism (rise/decay time)	4.1–5.2	s
<i>Gliotransmission</i>		
Presynaptic pathway (glutamate, release-increasing)		
Rise time	>0.05–28.3	s
Decay time	5.9–95.7	s
Presynaptic pathway (purines, release-decreasing)		
Rise time	1.6–8.2	s
Decay time	8.2–12	s
Postsynaptic pathway		
LTP rate (D-serine)	0.3–4.0	$\Delta\%/min$
TNF α -mediated AMPA receptor variation	± 5 –12	$\Delta\%/min$
TNF α -mediated GABA _A receptor variation	–0.3–0.7	$\Delta\%/min$
<i>Ion homeostasis</i>		
K ⁺ buffering		
Rise time	0.8–5.1	s
Decay time	3.9–18.6	s
Propagation	>30	$\mu\text{m/s}$
Na ⁺ spatial buffering	>2–80	$\mu\text{m/s}$

continued on the next page

Table 1. *continued*

Description	Range	Units
<i>Vascular coupling</i>		
Vasodilation		
Max % variation upon astrocytic Ca ²⁺ stimulation	5–8	Δ%
Percentage vessel diameter change rate	>0.05–0.37	Δ%/min
Vasoconstriction		
Max % variation upon astrocytic Ca ²⁺ stimulation	9–27.5	Δ%
Percentage vessel diameter change rate	1.6–1.7	Δ%/s
Onset delay from astrocyte activation	<1–3	s

References

- Allam SL, Ghaderi VS, Bouteiller JMC, Legendre A, Nicolas A, Greget R, Bischoff S, Baudry M, Berger TW (2012) A computational model to investigate astrocytic glutamate uptake influence on synaptic transmission and neuronal spiking. *Frontiers in Computational Neuroscience* 6:70
- Allaman I, Belanger M, Magistretti PJ (2011) Astrocyte–neuron metabolic relationships: for better and for worse. *Trends in Neurosciences* 34(2):76–87
- Allen NJ (2013) Role of glia in developmental synapse formation. *Current Opinion in Neurobiology* 23(6):1027–1033
- Alvarellos-González A, Pazos A, Porto-Pazos AB (2012) Computational models of neuron-astrocyte interactions lead to improved efficacy in the performance of neural networks. *Computational and mathematical methods in medicine* 2012:476,324
- Amzica F, Massimini M, Manfridi A (2002) Spatial buffering during slow and paroxysmal sleep oscillations in cortical networks of glial cells in vivo. *Journal of Neuroscience* 22(3):1042–1053
- Anderson WD, Makadia HK, Greenhalgh AD, Schwaber JS, David S, Vadigepalli R (2015) Computational modeling of cytokine signaling in microglia. *Molecular BioSystems* 11(12):3332–3346
- Arancibia-Carcamo IL, Ford MC, Cossell L, Ishida K, Tohyama K, Attwell D (2017) Node of Ranvier length as a potential regulator of myelinated axon conduction speed. *eLife* 6:e23,329
- Araque A, Parpura V, Sanzgiri RP, Haydon PG (1998) Glutamate-dependent astrocyte modulation of synaptic transmission between cultured hippocampal neurons. *Eur J Neurosci* 10:2129–2142
- Araque A, Carmignoto G, Haydon PG, Oliet SHR, Robitaille R, Volterra A (2014) Gliotransmitters travel in time and space. *Neuron* 81(4):728–739
- Attwell D, Buchan AM, Charpak S, Lauritzen M, MacVicar BA, Newman EA (2010) Glial and neuronal control of brain blood flow. *Nature* 468(7321):232–243
- Bains JS, Oliet SHR (2007) Glia: they make your memories stick! *Trends Neurosci* 30(8):417–424
- Barbour B (2001) An evaluation of synapse independence. *J Neurosci* 21(20):7969–7984
- Bazargani N, Attwell D (2016) Astrocyte calcium signaling: the third wave. *Nature Neuroscience* 19(2):182–189
- Bazhenov M, Timofeev I, Steriade M, Sejnowski TJ (2004) Potassium model for slow (2–3 Hz) in vivo neocortical paroxysmal oscillations. *Journal of Neurophysiology* 92(2):1116–1132
- Beattie E, Stellwagen D, Morishita W, Bresnahan J, Ha B, Von Zastrow M, Beattie M, Malenka R (2002) Control of synaptic strength by glial TNF α . *Science* 295(5563):2282–2285
- Bezzi P, Domercq M, Brambilla L, Galli R, Schols D, De Clercq E, Vescovi A, Bagetta G, Kollias G, Meldolesi J, Volterra A (2001) CXCR4-activated astrocyte glutamate release via TNF α : amplification by microglia triggers neurotoxicity. *Nat Neurosci* 4(7):702–710

- Bienenstock E, Cooper L, Munro P (1982) Theory for the development of neuron selectivity: orientation specificity and binocular interaction in visual cortex. *J Neurosci* 2(1):32–48
- Bindocci E, Savtchouk I, Liaudet N, Becker D, Carriero A, Gand Volterra (2017) Three-dimensional Ca^{2+} imaging advances understanding of astrocyte biology. *Science* 356:6339, DOI 10.1126/science.aai8185
- Brawek B, Garaschuk O (2017) Monitoring *in vivo* function of cortical microglia. *Cell Calcium* 64:109–117
- Brawek B, Liang Y, Savitska D, Li K, Fomin-Thunemann N, Kovalchuk Y, Zirdum E, Jakobsson J, Garaschuk O (2017) A new approach for ratiometric *in vivo* calcium imaging of microglia. *Scientific Reports* 7(1):6030
- Brea J, Senn W, Pfister JP (2013) Matching recall and storage in sequence learning with spiking neural networks. *The Journal of Neuroscience* 33(23):9565–9575
- Breslin K, Wade JJ, Wong-Lin K, Harkin J, Flanagan B, Van Zalinge H, Hall S, Walker M, Verkhatsky A, McDaid L (2018) Potassium and sodium microdomains in thin astroglial processes: A computational model study. *PLoS Computational Biology* 14(5):e1006151
- Bullock T, Horridge GA (1965) Structure and function in the nervous systems of invertebrates. Freeman, San Francisco
- Bushong EA, Martone ME, Jones YZ, Ellisman MH (2002) Protoplasmic astrocyte in CA1 stratum radiatum occupy separate anatomical domains. *J Neurosci* 22(1):183–192
- Butt AM (2013) Neuroglia, Oxford University Press, chap Structure and function of oligodendrocytes, pp 62–73
- Carr CE, Konishi M (1990) A circuit for detection of interaural time differences in the brain stem of the barn owl. *Journal of Neuroscience* 10(10):3227–3246
- Carr CE, Soares D (2002) Evolutionary convergence and shared computational principles in the auditory system. *Brain, Behavior and Evolution* 59(5-6):294–311
- Carr CE, Soares D, Parameshwaran S, Perney T (2001) Evolution and development of time coding systems. *Current Opinion in Neurobiology* 11(6):727–733
- Castro MA, Beltrán FA, Brauchi S, Concha II (2009) A metabolic switch in brain: glucose and lactate metabolism modulation by ascorbic acid. *Journal of neurochemistry* 110(2):423–440
- Chao CC, Hu S, Sheng WS, Peterson PK (1995) Tumor necrosis factor- α production by human fetal microglial cells: regulation by other cytokines. *Developmental Neuroscience* 17(2):97–105
- Chao TI, Rickmann M, Wolff JR (2002) The synapse-astrocyte boundary: an anatomical basis for an integrative role of glia in synaptic transmission. In: Volterra A, Magistretti PJ, Haydon PG (eds) *The Tripartite Synapse: Glia in Synaptic Transmission*, Oxford University Press, New York, chap 1, pp 3–23
- Chen N, Sugihara H, Sharma J, Perea G, Petracicz J, Le C, Sur M (2012) Nucleus basalis enabled stimulus specific plasticity in the visual cortex is mediated by astrocytes. *Proc Natl Acad Sci USA* 109(41):E2832–E2841, DOI 10.1073/pnas.1206557109

- Chever O, Djukic B, McCarthy KD, Amzica F (2010) Implication of Kir4.1 channel in excess potassium clearance: an in vivo study on anesthetized glial-conditional Kir4.1 knock-out mice. *Journal of Neuroscience* 30(47):15,769–15,777
- Chvátal A, Anděrová M, Kirchhoff F (2007) Three-dimensional confocal morphometry—a new approach for studying dynamic changes in cell morphology in brain slices. *Journal of Anatomy* 210(6):671–683
- Clarke LE, Barres BA (2013) Emerging roles of astrocytes in neural circuit development. *Nature Reviews Neuroscience* 14(5):311–321
- Clements JD (1996) Transmitter timecourse in the synaptic cleft: its role in central synaptic function. *Trends Neurosci* 19(5):163–171
- Covelo A, Araque A (2018) Neuronal activity determines distinct gliotransmitter release from a single astrocyte. *eLife* 7:e32,237
- Cui Y, Yang Y, Ni Z, Dong Y, Cai G, Foncelle A, Ma S, Sang K, Tang S, Li Y, Berry H, Shengzi W, Hailan H (2018) Astroglial Kir4.1 in the lateral habenula drives neuronal bursts in depression. *Nature* 554(7692):323
- D’Ambrosio R, Gordon DS, Winn HR (2002) Differential role of KIR channel and Na⁺/K⁺-pump in the regulation of extracellular K⁺ in rat hippocampus. *Journal of Neurophysiology* 87(1):87–102
- Danbolt NC (2001) Glutamate uptake. *Progress Neurobiol* 65:1–105
- Danbolt NC, Lehre KP, Dehnes Y, Ullensvang K (2002) Transporters for synaptic transmitter on the glial cell plasma membrane. In: Volterra A, Magistretti PJ, Haydon PG (eds) *The Tripartite Synapse: Glia in Synaptic Transmission*, Oxford University Press, New York, chap 1, pp 47–61
- De Pittà M, Brunel N (2016) Modulation of synaptic plasticity by glutamatergic gliotransmission: A modeling study. *Neural Plasticity* p 7607924
- De Pittà M, Volman V, Berry H, Ben-Jacob E (2011) A tale of two stories: astrocyte regulation of synaptic depression and facilitation. *PLoS Comput Biol* 7(12):e1002,293, DOI 10.1371/journal.pcbi.1002293, URL <http://dx.doi.org/10.1371%2Fjournal.pcbi.1002293>
- De Pittà M, Brunel N, Volterra A (2015) Astrocytes: orchestrating synaptic plasticity? *Neuroscience*
- De Pittà M (2019) Gliotransmitter exocytosis and its consequences on synaptic transmission. In: De Pittà M, Berry H (eds) *Computational Glioscience*, Springer, chap 10, pp 245–287
- De Pittà M, Berry H (2019a) *Computational Glioscience*. Springer
- De Pittà M, Berry H (2019b) A neuron–glial perspective for Computational Neuroscience. In: De Pittà M, Berry H (eds) *Computational Glioscience*, Springer, chap 1, pp 3–35
- Debanne D, Campanac E, Bialowas A, Carlier E, Alcaraz G (2011) Axon physiology. *Physiological Reviews* 91(2):555–602
- Deitmer JW, Rose CR (1996) pH regulation and proton signalling by glial cells. *Progress in Neurobiology* 48(2):73–103

- Di Castro M, Chuquet J, Liaudet N, Bhaukaurally K, Santello M, Bouvier D, Tiret P, Volterra A (2011) Local Ca^{2+} detection and modulation of synaptic release by astrocytes. *Nat Neurosci* 14:1276–1284, DOI 10.1038/nn.2929
- Diamond JS (2005) Deriving the glutamate clearance time course from transporter currents in CA1 hippocampal astrocytes: transmitter uptake gets faster during development. *J Neurosci* 25(11):2906–2916
- Dringen R (2000) Metabolism and functions of glutathione in brain. *Progress in Neurobiology* 62(6):649–671
- Durkee CA, Covelo A, Lines J, Kofuji P, Aguilar J, Araque A (2019) G_{mipr}/o protein-coupled receptors inhibit neurons but activate astrocytes and stimulate gliotransmission. *Glia* 67(6):1076–1093
- Ermentrout GB, Terman DH (2010) *Mathematical foundations of Neuroscience*. Springer, New York, NY
- Eroglu C, Barres BA (2010) Regulation of synaptic connectivity by glia. *Nature* 468(7321):223–231
- Fellin T, Pascual O, Gobbo S, Pozzan T, Haydon PG, Carmignoto G (2004) Neuronal synchrony mediated by astrocytic glutamate through activation of extrasynaptic NMDA receptors. *Neuron* 43:729–743
- Fields RD (2008) White matter in learning, cognition and psychiatric disorders. *Trends in Neurosciences* 31(7):361–370
- Fields RD, Woo DH, Basser PJ (2015) Glial regulation of the neuronal connectome through local and long-distant communication. *Neuron* 86(2):374–386
- FitzHugh R (1962) Computation of impulse initiation and saltatory conduction in a myelinated nerve fiber. *Biophysical Journal* 2(1):11–21
- Flanagan B, McDaid L, Wade J, Wong-Lin K, Harkin J (2018) A computational study of astrocytic glutamate influence on post-synaptic neuronal excitability. *PLoS computational biology* 14(4)
- Florence CM, Baillie LD, Mulligan SJ (2012) Dynamic volume changes in astrocytes are an intrinsic phenomenon mediated by bicarbonate ion flux. *PLoS One* 7(11):e51,124
- Ford MC, Alexandrova O, Cossell L, Stange-Marten A, Sinclair J, Kopp-Scheinpflug C, Pecka M, Attwell D, Grothe B (2015) Tuning of Ranvier node and internode properties in myelinated axons to adjust action potential timing. *Nature Communications* 6:8073
- Fourcaud-Trocmé N, Hansel D, van Vreeswijk C, Brunel N (2003) How spike generation mechanisms determine the neuronal response to fluctuating inputs. *J Neurosci* 23(37):11,628–11,640
- Franze K, Grosche J, Skatchkov SN, Schinkinger S, Foja C, Schild D, Uckermann O, Travis K, Reichenbach A, Guck J (2007) Müller cells are living optical fibers in the vertebrate retina. *Proceedings of the National Academy of Sciences* 104(20):8287–8292
- Funahashi S, Bruce CJ, Goldman-Rakic PS (1989) Mnemonic coding of visual space in the monkey’s dorsolateral prefrontal cortex. *Journal of Neurophysiology* 61(2):331–349

- Garnier A, Vidal A, Benali H (2016) A theoretical study on the role of astrocytic activity in neuronal hyperexcitability by a novel neuron-glia mass model. *The Journal of Mathematical Neuroscience* 6(1):10
- Gerstner W, Kistler WM (2002) Mathematical formulations of Hebbian learning. *Biological Cybernetics* 87(5-6):404–415
- Goldman L, Albus JS (1968) Computation of impulse conduction in myelinated fibers; theoretical basis of the velocity-diameter relation. *Biophysical Journal* 8(5):596–607
- Goldman-Rakic PS (1995) Cellular basis of working memory. *Neuron* 14(3):477–485
- Gordon G, Baimoukhametova D, Hewitt S, Rajapaksha W, Fisher T, Bains J (2005) Norepinephrine triggers release of glial ATP to increase postsynaptic efficacy. *Nat Neurosci* 8(8):1078–1086
- Gordon GRJ, Choi HB, Rungta RL, Ellis-Davies GCR, MacVicar BA (2008) Brain metabolism dictates the polarity of astrocyte control over arterioles. *Nature* 456(7223):745
- Götz M (2013) *Neuroglia*, Oxford University Press, chap Radial glial cells, pp 50–61
- Haber M, Zhou L, Murai KK (2006) Cooperative astrocyte and dendritic spine dynamics at hippocampal excitatory synapses. *J Neurosci* 26(35):8881–8891
- Halassa MM, Fellin T, Takano H, Dong JH, Haydon PG (2007) Synaptic islands defined by the territory of a single astrocyte. *J Neurosci* 27(24):6473–6477
- Halter JA, Clark Jr JW (1991) A distributed-parameter model of the myelinated nerve fiber. *Journal of Theoretical Biology* 148(3):345–382
- Hama K, Arii T, Katayama E, Martone M, Ellisman MH (2004) Tri-dimensional morphometric analysis of astrocytic processes with high voltage electron microscopy of thick Golgi preparations. *Journal of Neurocytology* 33:277–285
- Han X, Chen M, Wang F, Windrem M, Wang S, Shanz S, Xu Q, Oberheim NA, Bekar L, Betstadt S, Silva AJ, Takano T, Goldman SA, Nedergaard M (2013) Forebrain engraftment by human glial progenitor cells enhances synaptic plasticity and learning in adult mice. *Cell Stem Cell* 12(3):342–353
- Hartline DK (2011) The evolutionary origins of glia. *Glia* 59(9):1215–1236
- Henneberger C, Papouin T, Oliet SHR, Rusakov DA (2010) Long-term potentiation depends on release of D-serine from astrocytes. *Nature* 463:232–237
- Herculano-Houzel S (2014) The glia/neuron ratio: how it varies uniformly across brain structures and species and what that means for brain physiology and evolution. *Glia* 62(9):1377–1391
- Hirase H, Qian L, Barthó P, Buzsáki G (2004) Calcium dynamics of cortical astrocytic networks *in vivo*. *PLoS Biol* 2(4):0494–0496
- Hua JY, Smith SJ (2004) Neural activity and the dynamics of central nervous system development. *Nature Neuroscience* 7(4):327
- Huang YH, Bergles DE (2004) Glutamate transporters bring competition to the synapse. *Current Opinion in Neurobiology* 14(3):346–352

- Hughes EG, Orthmann-Murphy JL, Langseth AJ, Bergles DE (2018) Myelin remodeling through experience-dependent oligodendrogenesis in the adult somatosensory cortex. *Nature Neuroscience* 21:696–706
- Jadhav AP, Roesch K, Cepko CL (2009) Development and neurogenic potential of müller glial cells in the vertebrate retina. *Progress in retinal and eye research* 28(4):249–262
- James G, Butt AM (2001) P2X and P2Y purinoreceptors mediate ATP-evoked calcium signalling in optic nerve glia *in situ*. *Cell calcium* 30(4):251–259
- Kakegawa W, Miyoshi Y, Hamase K, Matsuda S, Matsuda K, Kohda K, Emi K, Motohashi J, Konno R, Zaitso K, Yuzaki M (2011) D-Serine regulates cerebellar LTD and motor coordination through the $\delta 2$ glutamate receptor. *Nature Neuroscience* 14(5):603–611
- Kaneko M, Stellwagen D, Malenka RC, Stryker MP (2008) Tumor necrosis factor- α mediates one component of competitive, experience-dependent plasticity in developing visual cortex. *Neuron* 58:673–680
- Kaschube M, Schnabel M, Löwel S, Coppola DM, White LE, Wolf F (2010) Universality in the evolution of orientation columns in the visual cortex. *Science* 330(6007):1113–1116
- Kasthuri N, Hayworth K, Berger DR, Schalek RL, Conchello JA, Knowles-Barley S, Lee D, Vázquez-Reina A, Kaynig V, Jones TR, Roberts M, Lyskowski JM, Tapia HS J C Seung, Roncal WG, Vogelstein JT, Burns R, Sussman DL, Priebe CE, Pfister H, Lichtman JW (2015) Saturated reconstruction of a volume of neocortex. *Cell* 162(3):648–661
- Kettenmann H, Ransom BR (2013) *Neuroglia*, 3rd edn. Oxford University Press
- Kettenmann H, Kirchhoff F, Verkhratsky A (2013) Microglia: new roles for the synaptic stripper. *Neuron* 77(1):10–18
- Kimura F, Itami C (2009) Myelination and isochronicity in neural networks. *Frontiers in Neuroanatomy* 3:12
- Kinney GA, Spain WJ (2002) Synaptically evoked GABA transporter currents in neocortical glia. *Journal of Neurophysiology* 88(6):2899–2908
- Kinney JP, Spacek J, Bartol TM, Bajaj CL, Harris KM, Sejnowski TJ (2013) Extracellular sheets and tunnels modulate glutamate diffusion in hippocampal neuropil. *Journal of Comparative Neurology* 521(2):448–464
- Kirov SA, Sorra KE, Harris KM (1999) Slices have more synapses than perfusion-fixed hippocampus from both young and mature rats. *Journal of Neuroscience* 19(8):2876–2886
- Kisvárdy ZF, Toth E, Rausch M, Eysel UT (1997) Orientation-specific relationship between populations of excitatory and inhibitory lateral connections in the visual cortex of the cat. *Cerebral cortex* 7(7):605–618
- Kofuji P, Newman EA (2004) Potassium buffering in the central nervous system. *Neuroscience* 129(4):1043–1054
- Kuga N, Sasaki T, Takahara Y, Matsuki N, Ikegaya Y (2011) Large-scale calcium waves traveling through astrocytic networks *in vivo*. *J Neurosci* 31(7):2607–2614

- Labin AM, Ribak EN (2010) Retinal glial cells enhance human vision acuity. *Physical Review Letters* 104(15):158,102
- Labin AM, Safuri SK, Ribak EN, Perlman I (2014) Müller cells separate between wavelengths to improve day vision with minimal effect upon night vision. *Nature Communications* 5:4319
- Laming PR, Kimelberg H, Robinson S, Salm A, Hawrylak N, Müller C, Roots B, Ng K (2000) Neuronal-glia interactions and behaviour. *Neurosci Biobehav Rev* 24:295–340
- Langer J, Stephan J, Theis M, Rose CR (2012) Gap junctions mediate intercellular spread of sodium between hippocampal astrocytes in situ. *Glia* 60(2):239–252
- Larsen BR, Assentoft M, Cotrina ML, Hua SZ, Nedergaard M, Kaila K, Voipio J, MacAulay N (2014) Contributions of the Na⁺/K⁺-ATPase, NKCC1, and Kir4.1 to hippocampal K⁺ clearance and volume responses. *Glia* 62(4):608–622
- Larter R, Craig MG (2005) Glutamate-induced glutamate release: a proposed mechanism for calcium bursting in astrocytes. *Chaos* 15:047,511
- Lawson LJ, Perry VH, Dri P, Gordon S (1990) Heterogeneity in the distribution and morphology of microglia in the normal adult mouse brain. *Neuroscience* 39(1):151–170
- Le Meur K, Mendizabal-Zubiaga J, Grandes P, Audinat E (2012) GABA release by hippocampal astrocytes. *Front Comp Neurosci* 6
- Lewitus GM, Pribiag H, Duseja R, St-Hilaire M, Stellwagen D (2014) An adaptive role of TNF α in the regulation of striatal synapses. *Journal of Neuroscience* 34(18):6146–6155
- López-Hidalgo M, Hoover WB, Schummers J (2016) Spatial organization of astrocytes in ferret visual cortex. *Journal of Comparative Neurology* 524(17):3561–3576
- Markram H, Lübke J, Frotscher M, Roth A, Sakmann B (1997) Physiology and anatomy of synaptic connections between thick tufted pyramidal neurones in the developing rat neocortex. *The Journal of Physiology* 500(2):409–440
- Masland RH (2001) The fundamental plan of the retina. *Nature Neuroscience* 4(9):877
- Mathiisen TM, Lehre KP, Danbolt NC, Ottersen OP (2010) The perivascular astroglial sheath provides a complete covering of the brain microvessels: an electron microscopic 3D reconstruction. *Glia* 58(9):1094–1103
- Matsuzaki M, Ellis-Davies G, Nemoto T, Miyashita Y, Iino M, Kasai H (2001) Dendritic spine geometry is critical for AMPA receptor expression in hippocampal CA1 pyramidal neurons. *Nat Neurosci* 4(11):1086–1092
- Matyash V, Kettenmann H (2010) Heterogeneity in astrocyte morphology and physiology. *Brain Res Rev* 63(1-2):2–10
- May JM (2012) Vitamin C transport and its role in the central nervous system. In: Stanger O (ed) *Water Soluble Vitamins*, Springer, Dordrecht, pp 85–103
- McAlpine D, Grothe B (2003) Sound localization and delay lines—do mammals fit the model? *Trends in Neurosciences* 26(7):347–350

- McCormick DA, Shu Y, Hasenstaub A, Sanchez-Vives M, Badoual M, Bal T (2003) Persistent cortical activity: mechanisms of generation and effects on neuronal excitability. *Cerebral Cortex* 13(11):1219–1231
- Medvedev N, Popov V, Henneberger C, Kraev I, Rusakov DA, Stewart MG (2014) Glia selectively approach synapses on thin dendritic spines. *Phil Trans R Soc B* 369(1654):20140,047
- Mesejo P, Ibáñez O, Fernández-Blanco E, Cedrón F, Pazos A, Porto-Pazos AB (2015) Artificial neuron–glia networks learning approach based on cooperative coevolution. *International Journal of Neural Systems* 25(04):1550,012
- Molofsky AV, Kelley KW, Tsai HH, Redmond SA, Chang SM, Madireddy L, Chan JR, Baranzini SE, Ullian EM, Rowitch DH (2014) Astrocyte-encoded positional cues maintain sensorimotor circuit integrity. *Nature* 509(7499):189
- Moore JW, Joyner RW, Brill MH, Waxman SD, Najar-Joa M (1978) Simulations of conduction in uniform myelinated fibers. Relative sensitivity to changes in nodal and internodal parameters. *Biophysical Journal* 21(2):147–160
- Mulligan S, MacVicar B (2004) Calcium transients in astrocyte endfeet cause cerebrovascular constrictions. *Nature* 431(7005):195–199
- Navarrete M, Perea G, de Sevilla D, Gómez-Gonzalo M, Núñez A, Martín E, Araque A (2012) Astrocytes mediate *in vivo* cholinergic-induced synaptic plasticity. *PLoS Biol* 10(2):e1001,259
- Navarrete M, Díez A, Araque A (2014) Astrocytes in endocannabinoid signalling. *Philosophical Transactions of the Royal Society B: Biological Sciences* 369(1654):20130,599
- Nave KA (2010) Myelination and support of axonal integrity by glia. *Nature* 468(7321):244
- Nimmerjahn A, Kirchhoff F, Kerr JND, Helmchen F (2004) Sulforhodamine 101 as a specific marker of astroglia in the neocortex *in vivo*. *Nat Methods* 1:31–37
- Nimmerjahn A, Kirchhoff F, Helmchen F (2005) Resting microglial cells are highly dynamic surveillants of brain parenchyma *in vivo*. *Science* 308(5726):1314–1318
- Oberheim NA, Takano T, Han X, He W, Lin JHC, Wang F, Xu Q, Wyatt JD, Pilcher W, Ojemann JG, Ransom BR, Goldman SA, Nedergaard M (2009) Uniquely hominid features of adult human astrocytes. *J Neurosci* 29(10):3276–3287
- O’Connor DH, Wittenberg GM, Wang SSH (2005) Graded bidirectional synaptic plasticity is composed of switch-like unitary events. *Proceedings of the National Academy of Sciences* 102(27):9679–9684
- Ogata K, Kosaka T (2002) Structural and quantitative analysis of astrocytes in the mouse hippocampus. *Neuroscience* 113(1):221–233
- Ohki K, Chung S, Ch’ng YH, Kara P, Reid RC (2005) Functional imaging with cellular resolution reveals precise micro-architecture in visual cortex. *Nature* 433(7026):597
- Otsu Y, Couchman K, Lyons DG, Collot M, Agarwal A, Mallet JM, Pfrieger FW, Bergles DE, Charpak S (2015) Calcium dynamics in astrocyte processes during neurovascular coupling. *Nature Neuroscience* 18(2):210

- Øyehaug L, Østby I, Lloyd CM, Omholt SW, Einevoll GT (2012) Dependence of spontaneous neuronal firing and depolarisation block on astroglial membrane transport mechanisms. *Journal of Computational Neuroscience* 32(1):147–165
- Panatier A, Theodosis DT, Mothet JP, Touquet B, Pollegioni L, Poulain DA, Oliet SH (2006) Glia-derived D-serine controls nmda receptor activity and synaptic memory. *Cell* 125:775–784
- Pascual O, Ben Achour S, Rostaing P, Triller A, Bessis A (2011) Microglia activation triggers astrocyte-mediated modulation of excitatory neurotransmission. *Proceedings of the National Academy of Sciences* pp 1–9, DOI 10.1073/pnas.1111098109
- Pelvig DP, Pakkenberg H, Stark AK, Pakkenberg B (2008) Neocortical glial cell numbers in human brains. *Neurobiology of Aging* 29(11):1754–1762
- Perea G, Araque A (2007) Astrocytes potentiate transmitter release at single hippocampal synapses. *Science* 317:1083–1086
- Perea G, Yang A, Boyden ES, Sur M (2014) Optogenetic astrocyte activation modulates response selectivity of visual cortex neurons in vivo. *Nature Communications* 5:ncomms4262
- Perez-Alvarez A, Navarrete M, Covelo A, Martin ED, Araque A (2014) Structural and functional plasticity of astrocyte processes and dendritic spine interactions. *The Journal of Neuroscience* 34(38):12,738–12,744
- Philips RT, Sur M, Chakravarthy VS (2017) The influence of astrocytes on the width of orientation hypercolumns in visual cortex: A computational perspective. *PLoS Computational Biology* 13(10):e1005,785
- Porto-Pazos AB, Veiguela N, Mesejo P, Navarrete M, Alvarellos A, Ibáñez O, Pazos A, Araque A (2011) Artificial astrocytes improve neural network performance. *PloS one* 6(4):e19,109
- Pósfai B, Cserép C, Orsolits B, Dénes Á (2019) New insights into microglia–neuron interactions: A neuron’s perspective. *Neuroscience* 405:103–117
- Pribrag H, Stellwagen D (2013) TNF- α downregulates inhibitory neurotransmission through protein phosphatase 1-dependent trafficking of GABA_A receptors. *The Journal of Neuroscience* 33(40):15,879–15,893
- Ransom CB, Ransom BR, Sontheimer H (2000) Activity-dependent extracellular K⁺ accumulation in rat optic nerve: the role of glial and axonal Na⁺ pumps. *The Journal of physiology* 522(3):427–442
- Reichenbach A, Robinson SR (1995) Phylogenetic constraints on retinal organisation and development. *Progress in Retinal and Eye Research* 15(1):139–171
- Reichenbach A, Wolburg H (2013) *Neuroglia*, Oxford University Press, chap Astrocytes and ependymal glia, pp 35–49
- Reichenbach A, Derouiche A, Kirchhoff F (2010) Morphology and dynamics of perisynaptic glia. *Brain Research Reviews* 63(1):11–25
- Richardson AG, McIntyre CC, Grill WM (2000) Modelling the effects of electric fields on nerve fibres: influence of the myelin sheath. *Medical and Biological Engineering and Computing* 38(4):438–446

- Rothman DL, Behar KL, Hyder F, Shulman RG (2003) In vivo NMR studies of the glutamate neurotransmitter flux and neuroenergetics: implications for brain function. *Annual Review of Physiology* 65(1):401–427
- Rothstein JD, Dykes-Hoberg M, Pardo CA, Bristol LA, Jin L, Kuncl RW, Kanai Y, Hediger MA, Wang Y, Schielke JP, , Welty DF (1996) Knockout of glutamate transporters reveals a major role for astroglial transport in excitotoxicity and clearance of glutamate. *Neuron* 16(3):675–686
- Roxin A, Montbrió E (2011) How effective delays shape oscillatory dynamics in neuronal networks. *Physica D: Nonlinear Phenomena* 240(3):323–345
- Roxin A, Brunel N, Hansel D (2005) Role of delays in shaping spatiotemporal dynamics of neuronal activity in large networks. *Physical Review Letters* 94(23):238,103
- Rusakov DA (2015) Disentangling calcium-driven astrocyte physiology. *Nature Reviews Neuroscience* 16:226–233
- Sahlender DA, Savtchouk I, Volterra A (2014) What do we know about gliotransmitter release from astrocytes? *Phil Tran R Soc B* 369:20130,592
- Sanchez-Vives MV, McCormick DA (2000) Cellular and network mechanisms of rhythmic recurrent activity in neocortex. *Nature Neuroscience* 3(10):1027
- Santello M, Volterra A (2012) TNF α in synaptic function: switching gears. *Trends in Neurosci* 35(10):638–647, DOI 10.1016/j.bbr.2011.03.031
- Santello M, Bezzi P, Volterra A (2011) TNF α controls glutamatergic gliotransmission in the hippocampal dentate gyrus. *Neuron* 69:988–1001
- Sasaki T, Matsuki N, Ikegaya Y (2011) Action-potential modulation during axonal conduction. *Science* 331(6017):599–601
- Savin C, Triesch J, Meyer-Hermann M (2009) Epileptogenesis due to glia-mediated synaptic scaling. *Journal of The Royal Society Interface* 6(37):655–668
- Savtchenko LP, Rusakov DA (2014) Regulation of rhythm genesis by volume-limited, astroglia-like signals in neural networks. *Phil Trans Royal Soc B: Biological Sciences* 369(1654):20130,614
- Savtchouk I, Volterra A (2018) Gliotransmission: Beyond black-and-white. *Journal of Neuroscience* 38(1):14–25
- Scemes E, Giaume C (2006) Astrocyte calcium waves: What they are and what they do. *Glia* 54:716–725
- Schummers J, Yu H, Sur M (2008) Tuned responses of astrocytes and their influence on hemodynamic signals in the visual cortex. *Sci STKE* 320(5883):1638
- Seidl AH, Rubel EW, Harris DM (2010) Mechanisms for adjusting interaural time differences to achieve binaural coincidence detection. *Journal of Neuroscience* 30(1):70–80
- Seifert G, Steinhäuser C (2017) Heterogeneity and function of hippocampal macroglia. *Cell and Tissue Research* pp 1–18

- Seung HS, Lee DD, Reis BY, Tank DW (2000) The autapse: a simple illustration of short-term analog memory storage by tuned synaptic feedback. *Journal of Computational Neuroscience* 9(2):171–185
- Sibson NR, Dhankhar A, Mason GF, Behar KL, Rothman DL, Shulman RG (1997) *In vivo* ^{13}C NMR measurements of cerebral glutamine synthesis as evidence for glutamate–glutamine cycling. *Proceedings of the National Academy of Sciences* 94(6):2699–2704
- Somjen GG, Kager H, Wadman WJ (2008) Computer simulations of neuron-glia interactions mediated by ion flux. *Journal of Computational Neuroscience* 25(2):349–365
- Stassart R, Goebbels S, Nave KA (2013) *Neuroglia*, Oxford University Press, chap Factors controlling myelin formation, pp 555–572
- Steinmetz CC, Turrigiano GG (2010) Tumor necrosis factor- α signaling maintains the ability of cortical synapses to express synaptic scaling. *Journal of Neuroscience* 30(44):14,685–14,690
- Stellwagen D, Malenka RC (2006) Synaptic scaling mediated by glial TNF- α . *Nature* 440(7087):1054–1059
- Stellwagen D, Beattie EC, Seo JY, Malenka RC (2005) Differential regulation of AMPA receptor and GABA receptor trafficking by tumor necrosis factor- α . *J Neurosci* 25(12):3219–3228
- Stevens JLR, Law JS, Antolík J, Bednar JA (2013) Mechanisms for stable, robust, and adaptive development of orientation maps in the primary visual cortex. *Journal of Neuroscience* 33(40):15,747–15,766
- Stobart JL, Ferrari KD, Barrett MJP, Glück C, Stobart MJ, Zuend M, Weber B (2018) Cortical circuit activity evokes rapid astrocyte calcium signals on a similar timescale to neurons. *Neuron* 98:726–735
- Takata N, Mishima T, Hisatsune C, Nagai T, Ebisui E, Mikoshiba K, Hirase H (2011) Astrocyte calcium signaling transforms cholinergic modulation to cortical plasticity *in vivo*. *J Neurosci* 31(49):18,155–18,165
- Tang F, Lane S, Korsak A, Paton JFR, Gourine AV, Kasparov S, Teschemacher AG (2014) Lactate-mediated glia-neuronal signalling in the mammalian brain. *Nature Communications* 5:3284
- Tomassy GS, Berger DR, Chen H, Kasthuri N, Hayworth KJ, Vercelli A, Seung HS, Lichtman JW, Arlotta P (2014) Distinct profiles of myelin distribution along single axons of pyramidal neurons in the neocortex. *Science* 344(6181):319–324
- Tomassy GS, Dershowitz LB, Arlotta P (2016) Diversity matters: a revised guide to myelination. *Trends in Cell Biology* 26(2):135–147
- Toyozumi T, Kaneko M, Stryker MP, Miller KD (2014) Modeling the dynamic interaction of Hebbian and homeostatic plasticity. *Neuron* 84(2):497–510
- Tuchin V (2000) *Tissue Optics*. SPIE Press, Bellingham, WA
- Ullah G, Cressman Jr JR, Barreto E, Schiff SJ (2009) The influence of sodium and potassium dynamics on excitability, seizures, and the stability of persistent states: II. Network and glial dynamics. *Journal of computational neuroscience* 26(2):171–183

- Ullén F (2009) Is activity regulation of late myelination a plastic mechanism in the human nervous system? *Neuron Glia Biology* 5(1-2):29–34
- Ventura R, Harris KM (1999) Three-dimensional relationships between hippocampal synapses and astrocytes. *J Neurosci* 19(16):6897–6906
- Verkhatsky A, Nedergaard M (2016) The homeostatic astroglia emerges from evolutionary specialization of neural cells. *Phil Trans R Soc B* 371(1700):20150,428
- Volman V, Ben-Jacob E, Levine H (2007) The astrocyte as a gatekeeper of synaptic information transfer. *Neural Computation* 19:303–326
- Volman V, Bazhenov M, Sejnowski TJ (2013) Divide and conquer: functional segregation of synaptic inputs by astrocytic microdomains could alleviate paroxysmal activity following brain trauma. *PLoS Computational Biology* 9(1):e1002,856
- Volterra A, Liaudet N, Savtchouk I (2014) Astrocyte Ca^{2+} signalling: an unexpected complexity. *Nature Reviews Neuroscience* 15:327–334
- Wade JJ, McDaid LJ, Harkin J, Crunelli V, Kelso JAS (2011) Bidirectional coupling between astrocytes and neurons mediates learning and dynamic coordination in the brain: a multiple modeling approach. *PLoS One* 6(12):e29,445
- Wang F, Smith NA, Xu Q, Fujita T, Baba A, Matsuda T, Takano T, Bekar L, Nedergaard M (2012a) Astrocytes modulate neural network activity by Ca^{2+} -dependent uptake of extracellular K^+ . *Sci Signal* 5(218):ra26, DOI 10.1126/scisignal.2002334
- Wang F, Xu Q, Wang W, Takano T, Nedergaard M (2012b) Bergmann glia modulate cerebellar purkinje cell bistability via Ca^{2+} -dependent K^+ uptake. *Proc Natl Acad Sci USA* 109(20):7911–7916
- Wang X, Lou N, Xu Q, Tian GF, Peng WG, Han X, Kang J, Takano T, Nedergaard M (2006) Astrocytic Ca^{2+} signaling evoked by sensory stimulation *in vivo*. *Nat Neurosci* 9(6):816–823
- Waxman SG (1980) Determinants of conduction velocity in myelinated nerve fibers. *Muscle & Nerve* 3(2):141–150
- Wiesel TN (1982) Postnatal development of the visual cortex and the influence of environment. *Nature* 299(5884):583
- Winship I, Plaa N, Murphy T (2007) Rapid astrocyte calcium signals correlate with neuronal activity and onset of the hemodynamic response *in vivo*. *J Neurosci* 27(23):6268–6272
- Wu Y, Dissing-Olesen L, MacVicar BA, Stevens B (2015) Microglia: dynamic mediators of synapse development and plasticity. *Trends in Immunology* 36(10):605–613
- Xiang J, Ennis SR, Abdelkarim GE, Fujisawa M, Kawai N, Keep RF (2003) Glutamine transport at the blood–brain and blood–cerebrospinal fluid barriers. *Neurochemistry International* 43(4-5):279–288
- Yamazaki Y, Hozumi Y, Kaneko K, Sugihara T, Fujii S, Goto K, Kato H (2007) Modulatory effects of oligodendrocytes on the conduction velocity of action potentials along axons in the alveus of the rat hippocampal CA1 region. *Neuron Glia Biology* 3(4):325–334

- Yang Y, Ge W, Chen Y, Zhang Z, Shen W, Wu C, Poo M, Duan S (2003) Contribution of astrocytes to hippocampal long-term potentiation through release of d-serine. *Proc Natl Acad Sci USA* 100(25):15,194–15,199
- Zalc B, Colman DR (2000) Origins of vertebrate success. *Science* 288(5464):271–271
- Zenke F, Gerstner W, Ganguli S (2017) The temporal paradox of Hebbian learning and homeostatic plasticity. *Current Opinion in Neurobiology* 43:166–176
- Zhang Z, Gong N, Wang W, Xu L, Xu T (2008) Bell-shaped D-serine actions on hippocampal long-term depression and spatial memory retrieval. *Cerebral Cortex* 18(10):2391–2401
- Zonta M, Angulo MC, Gobbo S, Rosengarten B, Hossmann KA, Pozzan T, Carmignoto G (2003) Neuron-to-astrocyte signaling is central to the dynamic control of brain microcirculation. *Nat Neurosci* 6:43–40